Universidad Zaragoza
1542

Final Master Project

Magnetic nanoparticles immobilization on cell membranes mediated by cadherins for magnetic hyperthermia studies

Author

Christian Castro Hinojosa

Supervisors

Dr. Raluca M. Fratila

Dr. María Moros Caballero

Master in Quantitative Biotechnology
2018-2019

Abbreviations

AA: Amino acids

BALB/c3T3: Mouse fibroblast

BSA: Bovine Serum Albumine

DAPI: 4 ',6-diamidino-2-phenylindol

DLS: Dynamic Light Scattering

DMEM: Dulbecco's Modified Eagle Medium

DPBS: PBS 1X + $CaCl_2$ (0.9 mM) and $MgCl_2$ (0.5 mM)

EC: E-cadherin extracellular domain repeat

EDC: 1-ethyl-3-(3-dimethylaminopropyl)carbodiimide

EDTA: Ethylenediaminetetraacetic Acid

FBS: Fetal Bovine Serum

HRP: Horseradish peroxidase

IPTG: Isopropyl β-D-1-thiogalactopyranoside

LB: Lysogeny broth

MABG: Meta-aminobenzylguanidine

MDCK: Madin-Darby Canine Kidney cell line

MNPs: Magnetic nanoparticles

NTA: N_α,N_α-Bis(carboxymethyl)-L-lysine hydrate

OD: Optical density

PBS: Phosphate Buffered Saline

PC: Protein corona

PEG750: Polyethylene glycol MW:750 Da

PEG5000: Polyethylene glycol MW:5000 Da

PMAO: Poly(maleic anhydride-*alt*-1-octadecene)

SDS-PAGE: Sodium dodecyl sulphate-polyacrylamide gel electrophoresis

SSB: Borate buffered saline

TAMRA: Tetramethylrhodamine-cadaverine

TBE: Tris(hydroxymethyl)-aminomethane, borate, EDTA

TBST: Tris Buffered Saline 1X + 0.1% Tween 20

TIRON: 1,2-dihydroxybenzene-3,5-disulphonic acid

TRITC: Tetramethylrhodamine

W2A: E-cadherin mutated fragments replacing tryptophan (Trp2) by alanine.

WT: E-Cadherin fragments Wild type

Abstract

Magnetic nanoparticles (MNPs) have the ability to generate heat when exposed to an alternating magnetic field. In biomedicine this property can be exploited to study the effects of localized heat generation on cell membranes. For this purpose, it is essential to target the MNPs to specific cell membrane receptors and achieve a stable and long-lasting immobilization of the MNPs on the cell membrane. Several molecules can be used as vectors; however, a stable conjugation is often difficult to achieve. Herein we explore the use of E-cadherin membrane protein as a potential targeting tool to generate a stable immobilization of MNPs on the cell membrane, based on homophilic E-cadherin – E-cadherin interactions. MNPs (12 nm diameter) were functionalized with polyethylene glycol (PEG) chains (MW: 750 or 5000 Da) and a derivative of nitrilotriacetic acid (NTA-Cu^{2+}) in a single step using EDC chemistry; then, E-cadherin protein fragments (wild type: WT or mutant: W2A) were conjugated on the surface of the nanoparticles in an oriented manner through their histidine tail (His-tag), generating a protocol that could be easily adapted to any protein containing a His-tag in its structure. The cell-nanoparticle interactions were evaluated in Madin-Darby canine kidney (MDCK) and mouse fibroblast BALB/c3T3 cells, expressing and lacking E-cadherins respectively. The results obtained showed that the MNPs coated with a larger PEG decreased the extent of non-specific interaction with cells. On the other hand, when the MNPs were immobilized by the W2A mutant protein fragments, their interaction with the MDCK cells was lower in comparison with the one of the MNPs functionalized with WT fragments. Furthermore, in the case of BALB/c3T3 cells, lacking E-cadherins on their membranes, the interaction with the different types of MNPs did not show clear differences. These results suggested that the MNPs interact with MDCK cells through homophilic interactions; furthermore, the mutation present in the protein fragments W2A generates changes in the binding of nanomaterials to the cell membrane, which could be used in future studies to improve the specificity and stability of the MNPs immobilization on cell membrane.

Resumen

Las nanopartículas magnéticas (MNPs) poseen la capacidad de generar calor cuando son expuestas a un campo magnético alterno. En biomedicina esta propiedad puede ser aprovechada para la generación de calor localizado sobre las membranas celulares, siendo primordial dirigir las MNPs de una forma específica hacia la superficie de las células y lograr una unión estable en el tiempo con ellas. Diversas moléculas han sido utilizadas como vectores, sin embargo, una unión estable suele resultar difícil de obtener sin la modificación previa de la célula. En este trabajo se investiga la posibilidad de utilizar a la proteína de membrana E-cadherina como una potencial herramienta para vectorizar MNPs hacia la superficie de la superficie celular, basándonos en sus interacciones homofílicas, con el fin de generar una inmovilización estable sobre la membrana celular. Se han utilizado MNPs de óxido de hierro de 12 nm de diámetro que han sido funcionalizadas con cadenas de polietilenglicol (PEG) (MW: 750 o 5000 Da) y con un derivado de ácido nitrilotriacético (NTA-Cu^{2+}) en un solo paso; posteriormente, fragmentos de proteína E-cadherina (tipo salvaje: WT o mutante: W2A) han sido conjugados en la superficie de las nanopartículas de forma orientada a través de una cola de histidina, generando un protocolo con una posible adaptación directa a cualquier proteína que contenga una cola de histidina en su estructura. La interacción células-nanopartículas se evaluó utilizando células de riñón canino Madin-Darby (MDCK) y células y células de fibroblasto de ratón BALB/c3T3, que expresan o carecen de E cadherina respectivamente. Los resultados obtenidos mostraron que las MNPs recubiertas con un PEG más grande disminuyeron la interacción inespecífica con las células. Por otro lado, cuando las MNPs fueron inmovilizados mediante fragmentos de proteínas mutantes W2A, su interacción con las células MDCK fue menor en comparación con la presencia de los fragmentos WT. Además, en el caso de las células BALB/c3T3, que carecen de E-cadherinas en sus membranas, la interacción con los diferentes tipos de MNPs no mostró diferencias claras. Estos resultados sugirieren que las MNPs interactúan a través de interacciones homofílicas con las cadherinas de las células MDCK, y también que la mutación presente en el fragmento de proteína W2A genera cambios en la unión de las MNPs a la membrana celular, que podrían usarse para mejorar la especificidad y la estabilidad de la unión en trabajos futuros.

Index

Introduction

Nanobiotechnology

Nanotechnology is defined as the science involved in the design, synthesis, characterization and development of applications of materials or functional devices constructed in one, two or three dimensions, with a size between 0.1 and 100 nanometers (one billionth of a meter).[1,2] Nowadays, nanotechnology has ever-increasing applications in different fields such as electronics, optics, catalysis, environment, robotics or medicine, and has become one of the most promising scientific fields of the 21st century to generate new technologies.[3] Nanomaterials often have new electrical, optical, magnetical among others kind of properties and features that are different from the bulk material. Usually many of these features, as well as, the potential application of the nanomaterials are determined by their size, shape or composition, which currently can be controlled during the synthesis process.[1,4]

Another very interesting feature of nanomaterials is the fact that their size is similar to the one of many biomolecules. In this context, the combined use of nanomaterials with biomolecules such as oligonucleotides, peptides, proteins, enzymes, polysaccharides or lipids, has generated a new scientific field called nanomedicine, which has the potential to overcome some of the current limitations in the medicine field.[6,7] For instance, among the key advantages of the use of nanosystems in nanomedicine there are: (1) an improved drug bioavailability by enhancing its aqueous solubility, (ii) enhanced interaction with cell membranes and proteins as nanomaterials are similar in size, (iii) high surface area to conjugate high loads and multiple therapeutic agents, (iv) potential to engineer multifunctional platforms, (v) the possibility of achieving an active remote triggering of the drug release.[2,7,9] This makes nanomaterials very useful for many biomedical applications, such as, biosensing, optical imaging, drug/gene delivery or even, tissue engineering.[5,6,8]

Magnetic nanoparticles (MNPs)

Magnetic nanoparticles (MNP) are colloidal nanomaterials composed of magnetic metals such as iron, cobalt, nickel, metal alloys or metal oxides, which can be synthesized with controllable sizes and shapes.[9] Among the existing MNPs, those composed by iron oxides (typically magnetite or maghemite) have been of interest for biomedical applications, due to their magnetic properties and their biocompatibility.[7,10]

The MNPs have a rapid response to an external field, therefore their position can be easily controlled by placing them near to a magnet.[13] Moreover, below certain sizes, MNPs possess a

superparamagnetic behavior, which is particularly useful for biomedical applications.[7] Superparamagnetism is a phenomenon that appears in ferromagnetic or ferrimagnetic nanoparticles whose size is small enough to ensure that the MNPs have a single magnetic domain. In this case, when an external magnetic field is applied, the MNPs are magnetized and align with the magnetic field; when the field is removed, the MNPs do not present remanent magnetization. In the context of biomedical applications, this is very important in order to maintain the colloidal stability of the MNPs and avoid their aggregation, which could lead to vascular embolisms. [7,14]

Another interesting feature of some MNPs, is their ability to generate heat as response to the application of an external alternating magnetic field (AFM), a property known as magnetic hyperthermia (MH).[9,12] Magnetic hyperthermia is originated due to the capacity of the MNPs to transform magnetic energy into heat through two mechanisms: the friction caused by the MNPs rotation (Brownian relaxation) or the magnetic moment rotation within the particle (Neel relaxation).[7,15] The most widespread application of this phenomenon is in cancer treatment, as the heat generated by the MNPs leads to a rise in temperature above physiological values and can induce the death of tumoral cells, which are typically more sensitive to heat than the healthy ones.[7,9] The MNPs heat capacity depends on several factors, both intrinsic -MNP size, shape, chemical composition- and extrinsic -parameters of the applied AMF (such as frequency, amplitude and application time of the AMF) and MNPs environment-.[16]

In some particular cases, the heat generated by the MNPs does not trigger cellular death (by apoptosis or other cell death mechanisms), but other kind of cellular responses such as, the activation of intracellular signaling or enhancement of internalization processes among others.[16] This so called *sub-lethal hyperthermia*, can be an interesting tool to activate thermosensitive ion channels, to externally manipulate intracellular pathways or to study or modulate the biophysical properties of the cellular plasma membrane.[17] In this sense, our group is currently working on one of these unconventional applications of the MNPs-based *sub-lethal hyperthermia*, as a potential tool to induce the transient pores formation on cell membranes and study subtle changes in their fluidity and permeability. To achieve this goal, a crucial step is represented by the immobilization of the MNPs on the cell membranes. Thus, the present work is focused on the development of an immobilization strategy of MNPs on the cell membrane based on the use of cadherin-cadherin interactions.

Immobilization of MNPs on cells

The MNPs-cells interactions including immobilization of MNPs on the cell membrane, can activate different cellular responses, such as damage at the plasma membrane level, the renewal of surface

proteins or the activation of biochemical responses or internalization processes.[18] The latter is a key factor to retain the MNPs on the cell membrane for longer periods of time, necessary to carry out the magnetic hyperthermia studies. The activation of an internalization process depends strongly on the characteristics of the MNPs such as, shape, size, surface charge, hydrophobicity, aggregation or surface functionalization.[7,19] Thus, the design of the MNPs should be carried out carefully, in order not only to generate a successful immobilization, but also to prevents the premature internalization of the MNPs.[15,19]

During the design, nanomaterials are often labeled or coated by other molecules through a process generally known as functionalization.[5] Depending on the molecules functionalized on the MNPs surface, these last can acquire the ability to target to specific cellular biomarkers, a process known as active targeting.[9,20] This vectorization normally gives nanoparticles the ability to selectively bind to membrane receptors, but it can also allow their localization even at the level of specific organelles, such as nucleus or mitochondria.[20]

Several strategies have been developed to immobilize nanomaterials on cell membranes, however they can be divided into two main groups: a first one, in which both the cells and the nanoparticle surface are modified to display the corresponding receptor and linker, and a second one in which only the nanoparticle surface is modified.[20] In both approaches, the MNPs immobilization can be mediated by covalent bonds, or by non-covalent interactions such as protein-linker or protein-protein interactions.[21]

An example of the first approach consist of the incorporation of azide reporters on cell membranes by metabolic glycoengineering in order to then attach, cyclooctyne-functionalized MNPs through a covalent chemical reaction known as bioorthogonal "click" chemistry.[22] On the other hand, in the second approach molecules such as folic acid, transferrin, antibodies or sugars, as well as, synthetic moieties like meta-aminobenzylguanidine (MABG), have been used as linkers of specific cellular receptors. For instance, MABG molecules allowed to target nanoparticles to norepinephrine receptors overexpressed in neuroblastoma cells.[20,21] Other systems widely used are aptamers, chains of oligonucleotides that exhibit a characteristic three-dimensional structure capable to bind to specific membrane receptors of tumor cells.[23]

In all these cases it is important to take into account the nature and density of the functionalized molecules, as well as, the orientation of these molecules on the MNPs surface as important factors that can affect the MNPs interaction capabilities, which could determine a successful immobilization.[24,25] For example, the specific targeting of functionalized nanomaterials is a complicated process, as often can result in non-specific interactions within the biological environment, due to its complexity.[26] The

presence of several molecules such as, ions, lipids, sugars or proteins has been found to interact notably with the surface of almost any type of nanoparticles.[27,28]

The interactions of the nanoparticles with components of biological systems results in the formation of a so-called corona of biomolecules. The corona formed by proteins is denominated as protein corona (PC) and it is believed that its formation is inevitable for almost all the nanoparticles when placed in biological environments.[7] Nevertheless, it has been observed that a wide range of factors including the nanomaterial characteristics, the environment conditions or the interaction time could determine the formation and identity of the PC.[29] Thus in an attempt to avoid or reduce the PC formation, as well as, other non-specific interactions, BSA-like proteins or polymers such as polyethylene glycol (PEG) have been used to coat the MNPs hypothesizing that their presence could avoid or diminish the binding of other proteins.[30]

Lastly, the functionalization of MNPs with biomolecules such as antibodies or proteins can be performed in an oriented or in a non-oriented manner.[31] The non-oriented manner could result straightforward, however, an oriented functionalization which is often more challenging, could result to be more attractive to achieve better results during the MNPs immobilization.[32] The non-oriented union can promote a null or non-specific interaction with the target (Figure 1A), whilst, an oriented molecule makes more probable the interaction, because the union site is placed to be free and accessible.[32] The oriented approach is therefore the most convenient in order to take advantage of the small surface area of MNPs used for biomedical applications (Figure 1C).[33] On the contrary, when using larger particles such as microbeads, the large surface area can promote some degree of interaction even when some molecules are not oriented on their surface (Figure 1B).

Because all these reasons, among all the molecules and immobilization strategies mentioned before, we have focused on the use of a cellular-adhesion protein (E-cadherin) functionalized in an oriented manner to target the MNPs to the cadherins present in the cell membrane of living cells.

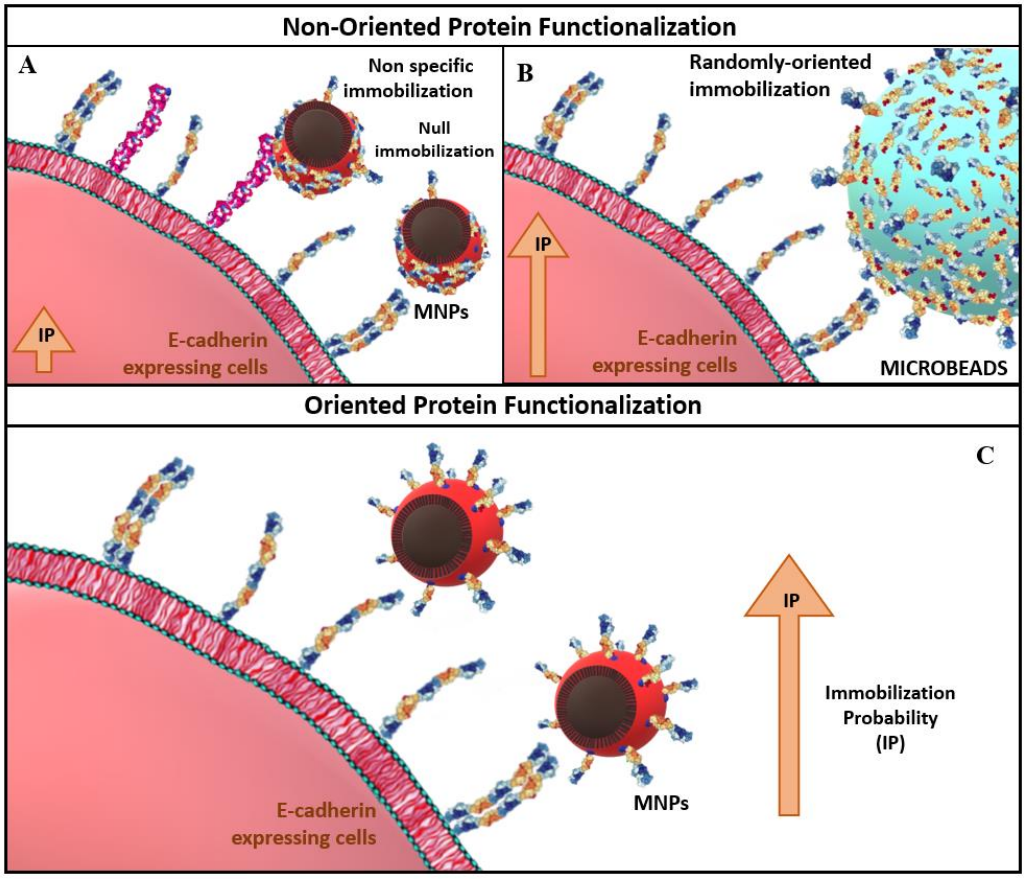

Figure 1: A: Immobilization on cell membranes of: MNPs functionalized with E-cadherin in a non-oriented manner. **B:** Immobilization on cell membranes of microbeads functionalized with E-cadherin in a non-oriented manner. **C:** Immobilization on cell membranes of MNPs functionalized with E-cadherin in an oriented manner.

Cadherin proteins as a tool to target cell membranes

Cadherins are a family of transmembrane proteins that constitute a part of the cell–cell adhesion machinery, and are particularly known for having a Ca^{2+}-dependent activity. These proteins are present in a quite variety of organisms and tissues, furthermore they play an essential role in processes such as tissue and organ morphogenesis, and also in homeostasis by controlling cell–cell adhesion and cell signaling processes. [34] Cadherins family consists of five major subfamilies, classical cadherins (type I), closely related cadherins (type II), desmosomal cadherins (desmocollins and desmogleins), proto-cadherins, and a variety of cadherin-related molecules.[34,35]

Type I cadherins are composed by three domains, an intracellular, a single trans-membrane section and an extracellular domain.[34] The extracellular portion is the section that interacts with other proteins, but mainly with cadherins of the same type a phenomenon known as homophilicity. This kind of interaction can even promote a homotypic behavior in cells (union only between identical cell types).[35]

E-cadherin is a type I cadherin mainly found in epithelial cells that has three domains, a cytoplasmic domain of about 150 amino acids (AA), a single transmembrane section and an ectodomain of about 550 AA involved in the homophilic interactions.[36] E-cadherin ectodomain comprises five extracellular repeat structures (EC1 to EC5) each one composed by approximately 110 AA and folded like an immunoglobulin domain.[37] Each repeat contains conserved motifs to maintain calcium-binding activity, in order to conserve the cell adhesion potential, avoid trypsin sensitivity and to stretch and turn more rigid the structure.[36,38]

The interaction of the MNPs developed in this work with the cadherins present on the cell membrane will be mediated by homophilic interactions, so it is important to understand how this interaction works. Different theories have been proposed attempting to explain this kind of union at molecular and cellular level. However, until now non conclusive model for E-cadherin homophilic interaction have been described,[36,39] although, all the models conserve as a common characteristic the importance of EC1 repeat to make possible the homophilic adhesion.[40]

In the EC1 repeat the first three amino acids of the N-terminal extreme (fully conserved among class I and II cadherins) also called adhesion arm, have a tryptophan residue at position 2 (Trp2) that is the key residue to perform a dimerization between E-cadherins from different cells, well known as *trans* dimerization (Figure 2A).[36] A *cis* dimerization also occurs between E-cadherins of the same cell, in this lateral interaction the backbone of the EC1 domain interacts with the EC2/EC3 domains of an adjacent cadherin, forming the E-cadherin *cis*-dimer.[41] Recent models suggest that this interaction is not determinant for the *trans*-dimerization occurrence, however as a *cis* dimerization triggers a clustering process recruiting more E-cadherins, it results to have a cooperative effect by increasing the probability of *trans*-dimer formation (Figure 2B).[41,42]

Nowadays the most accepted model for E-cadherin monomers interaction claims an interaction in two ways.[39] First, if the adhesion arm is in "open" conformation, Trp2 binds within the hydrophobic pocket of the opposing monomer and forms a strand-swapped dimer. On the other hand, in the "closed" conformation, Trp2 binds into the hydrophobic pocket of its own monomer, and the monomers form an adhesive unstable dimer mediated by inter-domain contacts, called X-dimer.[43] Nevertheless, studies suggest that X-dimer is a kinetic intermediate of the strand-swapped dimer (Figure 2C).[44] In addition, it is possible that an extra interaction state even more stable than swapped dimer called Y-dimer exists.[39]

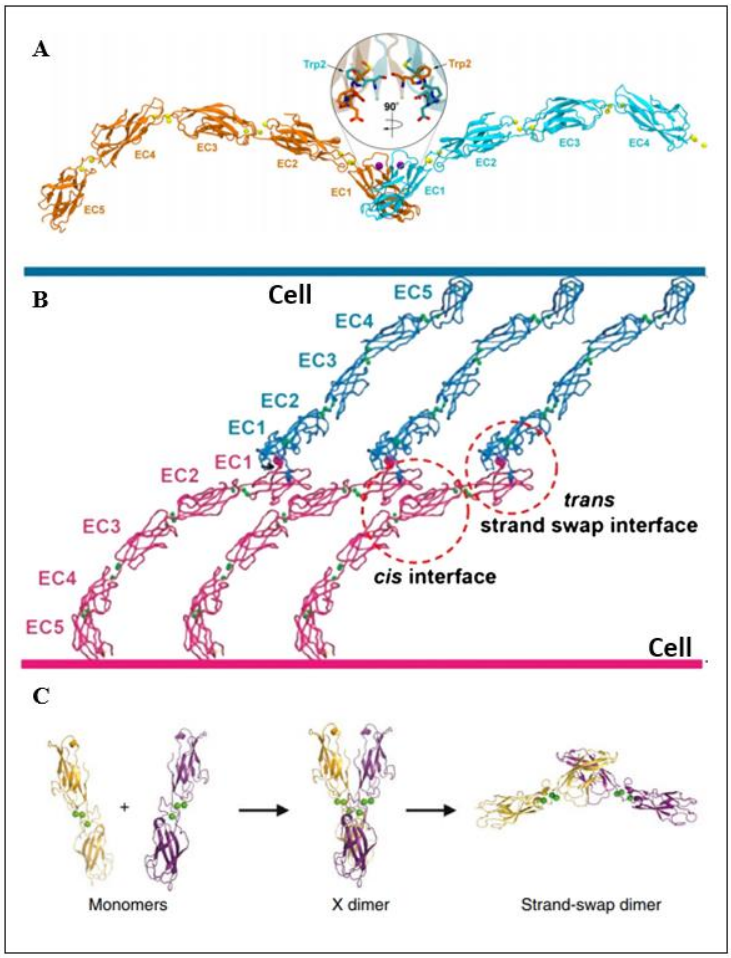

Figure 2: Interaction models of E-cadherin ectodomains. **A:** Strand-swap dimer in two completes ectodomains. **B:** Two-step adhesive binding by classical cadherins. Modified from:[39, 41, 43]

As we have noted Trp2 is essential to create a strong interaction between E-cadherin protein fragments, but if this amino acid or others residues that forms the hydrophobic pocket (i.e. Trp2 by Ala) are changed, the monomers are not able to reach a strand-swapped dimer conformation and are stabilized only as a X-dimer conformation.[43,45] Although it has been demonstrated that in addition to strand swapping, X-dimers are involved in cell-cell adhesion, it is possible that each dimer conformation activates different cellular response during the attachment of MNPs on the cell membrane. These variations could include changes in the processes of internalization that allow to maintain the MNPs on the cell membrane during longer times.[46] For this reason we proposed the functionalization of the MNPs with a wild type (WT) fragment EC1-EC2 and also with a fragment with the Trp2 replaced by an alanine, from now on referred to as W2A mutant.

Design of the MNPs

Different strategies to functionalize nanomaterials with proteins have been developed so far. Methods based on a covalent coupling have been described, such as the formation of amine bonds mediated by (1-ethyl-3-(3-dimethylaminopropyl)carbodiimide) (EDC) and N-hydroxysulfosuccinimide (sulfo-NHS), which generally produce a non-oriented functionalization.[47] Another method widely used is the biotin-avidin coupling, in which biotinylated proteins are coupled to MNPs functionalized with avidin or related molecules, favoring an oriented functionalization and also the reaction specificity. In this method, however, proteins have to be modified with biotin, which can increase economic costs. [48]

Nevertheless, another method less common and generally used in affinity columns or to functionalize surfaces has been described, consisting on the use of nitrilotriacetic acid (NTA) as NTA-Ni^{2+} or NTA-Cu^{2+} complexes that can further coordinate polyhistidine-tag (His-tags) sequences that can be cloned and expressed into a protein, allowing an oriented functionalization with a high reaction specificity.[47] As was mentioned before, despite being widely applied for other applications, such as purification columns, this method is not common to achieve an oriented functionalization of proteins on MNPs, resulting to be a novel functionalization strategy for the MNPs.

In addition to protein functionalization, is necessary to consider the MNPs coating with molecules that ensure their colloidal stability in biological media (for example, cell culture medium) and avoid non-specific interactions.[48] In general polymers such as, polyvinylpyrrolidone (PVP) or polyethylene glycol (PEG), among others, are used for this purpose because they have the capability to neutralize the MNPs surface charge, in a process known as passivation.[49]

Objectives

The general objective of this work is to immobilize magnetic nanoparticles on epithelial cell membranes mediated by homophilic interactions of E-cadherin proteins. In order to achieve this goal, the specific objectives are:

1. The optimization of the functionalization of magnetic nanoparticles with PEG and NTA-Cu^{2+} molecules.
2. The functionalization of the magnetic nanoparticles with E-cadherin protein fragments conjugated in an oriented manner.
3. The immobilization of the E-cadherin-functionalized magnetic nanoparticles on epithelial cell membranes.

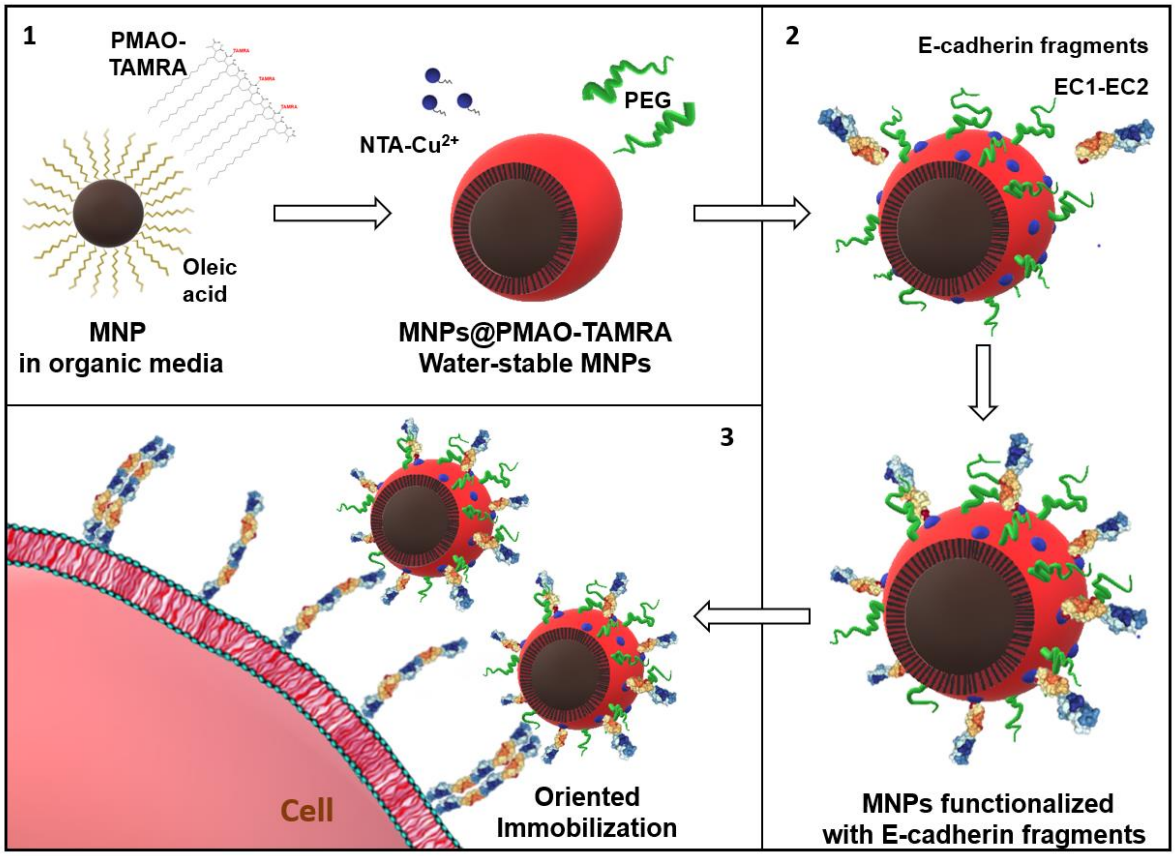

Figure 3: TFM Objectives

Experimental Section

E-cadherin protein fragments production

E-cadherin (EC1-EC2) expression

To express E-cadherin protein fragments (EC1-EC2, WT and W2A), 100 ml of lysogeny broth (LB) medium with kanamycin (50 µg/ml) were used to start a preculture of Escherichia coli BL21 containing a pET plasmid in which a EC1-EC2 gene was cloned, with a His-tag at the C-terminal end. The plasmid was kindly provided by Dr.Helene Feracci (CNRS, Bordeaux, France). The pre culture was incubated at 37 ºC under agitation overnight. After this time, a new larger culture of 250 ml was prepared diluting the first subculture until reaching a final optical density (O.D.) of 0.1. This new culture was incubated at 37 ºC until reaching an OD of 0.6. Once elapsed this time, the expression induced agent isopropyl β-D-1-thiogalactopyranoside (IPTG) was added, and the mixture was incubated during two hours at the same temperature. The culture was centrifuged at 500 x g for 20 min, at 4 ºC. The supernatant was removed and the pellet frozen until the posterior protein extraction.

E-cadherin extraction and purification

E-cadherin fragments expressed in E. coli forms inclusion bodies, thus, in order to extract and purify the protein it was necessary to denaturalize it using urea and then leaving it to refold by removing the denaturizing agent. The lysis buffer consists of urea (4 M), Na_2HPO_4 (50 mM), imidazole (20 mM), β-mercaptoethanol (20 mM) and a protease inhibitor (Protease Inhibitor Cocktail for use in purification of His-tagged proteins, Sigma-Aldrich, Ref: P8849). The pellet resultant from the previous step was resuspended in the lysis buffer in an ice bath (to avoid protease activity) and incubated at 4 ºC for 20 minutes under magnetic agitation. After this time, the suspension was centrifuged at 10000 x g for 30 minutes, and the pellet was discarded.

To purify the protein, it was attached to agarose beads containing an NTA derivative (N_α,N_α-Bis(carboxymethyl)-L-lysine hydrate) as NTA-Ni^{2+} complexes on its surface (QIAGEN, Ref. 30430), attaching the proteins by their His-tags. First, the beads were washed twice with urea buffer. Then, the supernatant obtained from a 250 ml of bacteria culture was incubated with 6 ml of agarose beads for 2 hours at 4 ºC in a rotating wheel. After that, the beads were centrifuged at 3000 x g for 15 minutes, the supernatant resultant was discarded and the beads were washed six times with buffer urea. After the washes, the beads were dialyzed against a decreasing urea gradient: 3 M, 2 M, 1 M, and finally several dialysis steps with PBS + β-mercaptoethanol were performed. The resultant beads containing the E-

cadherin fragments were stored at 4 °C in around 20 ml of PBS buffer with 0.05% sodium azide to avoid contamination with microorganisms or fungi.

Trypsin sensitivity assay

A correct E-cadherin fragments folding present resistance towards trypsin mediated cleavage in presence of Ca^{2+} due to structural modifications, on the other hand in the absence of Ca^{2+} the fragments are susceptible to proteolysis. Thus, a trypsin solution can be used to evaluate the correct folding of the protein obtained. To do this, the amount of agarose beads containing 30 µg of E-cad fragments were washed in buffers containing $CaCl_2$ (Ca^{2+} present) or EDTA (Ethylenediaminetetraacetic Acid) (Ca^{2+} absent). Then, the protein was eluted with imidazole (0.25 M) and each sample incubated with trypsin-agarose (Sigma, T4019-50UN). After 1 hour of incubation at 37 °C, the trypsin-agarose was removed through a miniSpin column filter and the resultant samples were loaded in a SDS-PAGE gel (4-15%, BioRad, 15 µl/well, 100V, 1 hour). and detected by using a blue coomassie staining.

Water transfer of hydrophobic MNPs[22]

First, 140 mg of PMAO (MW: 30-50 kDa) were dissolved in a round-bottomed flask with 15 ml of CH_3Cl. At the same time 2 mg of TAMRA were dissolved in absolute ethanol (1 mg/ml) and transferred to the flask, leaving the mixture under magnetic stirring at room temperature overnight, protected from light.

MNPs with a diameter of 12 nm, synthesized by thermal decomposition method, coated with oleic acid and dispersed in a hexane solution containing oleic acid and oleylamine were used as starting material.[22] Before the water transfer a washing step was performed, diluting 10 mg of MNPs solution in absolute ethanol and recovering them with a magnet during 3 minutes eliminating the supernatant. The MNPs were dispersed in hexane and diluted again in ethanol, repeating the process three times to eliminate the excess of oleylamine and oleic acid. In the last repetition MNPs were resuspended in 2 ml of CH_3Cl instead of hexane and the suspension was mixed with 81 ml of CH_3Cl and the PMAO-TAMRA solution.

The final mixture was sonicated for 15 minutes at room temperature, after this time the excess of CH_3Cl was evaporated using a rotary evaporator setting a pressure of 200 mbar at 40 °C until a final volume of 5-10 ml. Once eliminated the organic solvent, 15 ml of water and 15 ml of NaOH 0.1 N were added to the mixture simultaneously to hydrolyze the anhydride groups present in the PMAO and to confer stability in water to the MNPs. Remaining organic solvent was evaporated again under the

same conditions with pressure of 200 mbar and 70 °C until reaching a final volume of 10-20 ml. The suspension obtained was filtered using a Millipore filter (0.22 µm) to remove MNPs aggregates and unreacted polymer.

The excess of polymer was eliminated by four consecutive ultra-centrifugations at 70000 x g per 2 hours each one and the resultant nanoparticles suspension MNP@PMAO@TAMRA was stored at 4 °C in the dark. The MNPs concentration was measured following the method explained later and since now will be given as mg of iron per milliliter (mg Fe/ml).

Functionalization Strategies

Functionalization with polyethylene glycol (PEG)[15]

Two PEG molecules of different MW: 750 Da (PEG750) and 5000 Da (PEG5000), both with amine and methoxy end groups were used. Each PEG molecule and the coupling reagent EDC, were dissolved in different microtubes containing a borate buffered saline (SSB) solution (50 mM, pH 9).

For each functionalization, 1 mg of MNPs were mixed with either 22.26 µmols of PEG750 or 5.57 µmols of PEG5000 into a microtube. The mixture was warmed to 37 °C in the dark and 40 µmols of EDC were added in the same reaction tube twice, at time 0 and after 30 minutes, letting the mixture react for three hours and 30 minutes in total. Then, eight washes using ultra-centrifugal filters (Amicon, Millipore, 100 kDa cutoff) were performed to eliminate the excess of reagents.

Functionalization with NTA-Cu^{2+} molecules[15]

For this step, a modified NTA molecule which contains an extra tail ending in a primary amine group (NH_2) was used. 14.41 µmols of this modified NTA, since now only referred as NTA and 23,7 µmols of $CuSO_4$ were dissolved in 600 µl of buffer SSB pH 8, and the pH was adjusted to 10 using NaOH (6 N) to precipitate copper excess. Precipitation was accelerated through a centrifugation at 11300 x g for 5 min, after this time the supernatant was recovered and the pH readjusted to 9 using HCl (4 N). In a new microtube 0.33 mg of MNPs were mixed with NTA-Cu^{2+} solution. The mixture was warmed at 37 °C and 20 µmols of EDC were added in the same reaction tube twice, at time 0 and after 30 minutes, letting the mixture react for three hours and 30 minutes in total. Then, eight washes using ultra-centrifugal filters (Amicon, Millipore, 100 kDa cutoff) were performed to eliminate unreacted reagents.

One-pot functionalization with PEG and NTA-Cu^{2+}

A solution containing 14.41 µmols of NTA and 23,7 µmols of $CuSO_4$ was prepared in 500 µl of SSB solution (pH 8), the precipitation of copper excess was performed following the same protocol explained above. Another solution of either PEG750 (22.26 µmols) or PEG5000 (5.57 µmols) was prepared in 100 µl of SSB (pH 9). Both solutions were mixed and the final volume adjusted to 606 µl. Functionalization was performed adding to a new tube the equivalent to 0.33 mg of iron in nanoparticles together with NTA-Cu^{2+}-PEG solution. The mixture was warmed at 37 °C and 40 µmols of EDC dissolved in 20 µl of SSB buffer at pH 9 were added in the same reaction tube twice, at time 0 and after 30 minutes, letting the mixture react for three hours and 30 minutes in total. Then, eight washes using ultra-centrifugal filters (Amicon, Millipore, 100 kDa) were performed to eliminate unreacted reagents.

Functionalization with E-cadherin protein fragments

In an Eppendorf tube, 0.33 mg of MNPs were added and centrifuged for 2 hours at 25000 x g in order to match the starting volumes when working with more than one tube. During this time a solution of 33 µg of E-cadherin fragments EC1-EC2 (WT or W2A) in 660 µl of phosphate buffered saline (PBS) solution was prepared from a purified protein stock. As a control, an extra microtube was prepared adding also imidazole (0.25 M) to the protein solution. After centrifugation, the supernatant was eliminated and 660 µl of protein solution were added to the microtube. Functionalization was performed leaving the microtube in stirring in a horizontal shaker for one hour at 37 °C. After this time, another centrifugation was done with the previous conditions, the supernatant was collected and kept at 4 °C. The resulting pellet was sonicated at least 10 s and also kept at 4 °C.

Characterization techniques

Determination of Iron concentration

After all water transfers and after each functionalization step an iron determination was performed to know the mass available for further experiments.

To determine iron concentration, 50 µl of six different iron standard solutions (0, 100, 200, 400, 600, 800 µg Fe/ml) were prepared in microtubes in triplicate. Each sample of MNPs suspension of unknown concentration was prepared mixing 5 µl of MNPs and 45 µl of deionized water also in

triplicate. In all the microtubes 100 µl of aqua regia ($HCl:HNO_3$ 3:1) solution were added and the samples were warmed at 60 °C for 15 minutes. After this time, 350 µl of deionized water were added to all the microtubes and 50 µl of each mixture were transferred to a 96 well plate. In each well 100 µl of Na_3PO_4 (0.2M, pH 9.7), 50 µl of KOH (4 N) and 10 µl of Tiron (1,2-dihydroxybenzene-3,5-disulphonic acid) 0.25 M were added. After 15 minutes, iron concentration was measured in a spectrophotometer using a wavelength of 480 nm.

Gel Electrophoresis

In order to determine changes in the surface charge of the MNPs due to the diminishing of carboxyl groups availability, an electrophoresis was performed after each functionalization step. An agarose gel of 2% (m/v) was prepared using a tris(hydroxymethyl)-aminomethane, borate, EDTA (TBE) 0.5X buffer. Samples were mixed with glycerol 25% dissolved in TBE (0.5X), to get a final volume of 8 µl. Each sample was loaded by pipetting and conditions were set at 75 minutes and 120 V.

Furthermore, after each water transfer of MNPs an electrophoresis was performed to visualize using a UV filter differences of polymer concentrations between the supernatants recovered after the four ultracentrifugation steps using an agarose gel at 1% (m/v) and setting conditions at 50 minutes and 90 V.

DLS and ζ-potential

For each sample a solution of 0,05 mg Fe/ml was prepared using milli-Q water, 800 µl of the solution were sonicated during 10 seconds and added to a cuvette own of the equipment, both measurements were performed in a Zetasizer instrument from Malvern Panalytical, combining 5 runs per measurement at 25 °C. In the case of the ζ-potential, the dispersed light at an angle of 13° was measured. The data collected was analyzed using the Zetasizer software.

Dot-blot

Nitrocellulose membranes with a size of 1 cm^2 were placed in a 24-wells plate, one per sample. 3 µl of sample were added to each membrane and were left to dry during 30 minutes. Initial protein stock solution and PBS buffer were also added as controls. After this time 500 µl of blocking buffer TBST (Tris Buffered Saline (TBS) 1X + 0.1% Tween 20) + 2,5% bovine serum albumin (BSA), were added to each well and the plate was incubated at least 30 minutes at 37 °C. After blocking, a wash was

performed eliminating the liquid in each well, adding 500 µl of TBST without BSA and incubating for 5 min at 37 °C, repeating the process four times.

Anti-E-cadherin polyclonal antibody kindly provided by the PhD student (Bea Martín) and prepared in TBST with a concentration of 0.75 µg/ml and a solution of a commercial Anti-rabbit antibody raised in goat (Dako, Ref: P0448) were used. After the washes, 500 µl of anti-E-cadherin antibody were added to each well, incubated during 30 min at 37 °C and, four washes were performed again. The procedure was repeated after adding 500 µl of Anti-rabbit antibody, including four washes. After the last wash 70 µl of horseradish peroxidase (HRP) Substrate Luminol: HRP Substrate Peroxide, 1:1 (Immobilon Western. Ref. WBKLS0500) were added to each membrane and the results were visualized in a Chemidoc equipment from Bio-Rad.

Nanoparticles stability in DMEM medium

Microtubes containing functionalized MNPs were sonicated during 10 seconds, 20 µl of MNPs were mixed with 80 µl of PBS 1X procuring to adjust a final concentration of 0.1 mg Fe/ ml of solution. The mixture was filtered using a 0.22 µm diameter filter (Millipore) and in a multi-well plate 100 µl were mixed together with 100 µl of Dulbecco's modified eagle medium (DMEM) medium complete or without fetal bovine serum (FBS). Each well was observed using an inverted microscope after 15 minutes.

Cell Culture Techniques

Cell culture techniques, were performed in sterile conditions inside of a laminar flow hood. Madin-Darby Canine Kidney (MDCK) and BALB/c3T3 cell lines were grown in DMEM media (Gibco) supplemented with 10% fetal bovine serum (FBS), 1X glutaMAX (Gibco) and antibiotic penicillin-streptomycin (10,000 U/mL; Gibco, Ref: 15140122).

Cell culture and maintenance

Each passage to a new flask with new medium was performed once the cells reached at least 85% of confluence. To split the cells, all the medium was removed from the T25 culture flask, 5 ml of PBS were added to wash the remaining medium and were removed. 1 ml of trypsin solution was added to the flask and was incubated at 37 °C and 5% CO_2 atmosphere during 5 minutes. After this time the cells were detached, 3 ml of new medium was added, and cells were centrifuged at 300 x g for 5 minutes to collect the cells. All supernatant was discarded and the cells were resuspended in new

medium. Finally, cells were counted, diluted and transferred to a new flask, and were incubated at 37 °C in 5% CO_2 atmosphere.

Interaction of MNPs with cell membranes

MDCK or BALB/c3T3 cells were seeded at a density of 30000 or 10000 cells per well respectively in a 12-well µ-chamber (Ibidi), the cultures were incubated 24 hours at regular conditions of 5% CO_2 atmosphere and 37 °C. Meanwhile, the MNPs previously prepared were sterilized by filtration with a Millipore filter (0.22 µm diameter) and the resulting sterilized MNPs were diluted in DMEM medium reaching a final concentration of 100 µg Fe/ml.

The medium in each ibidi well was removed and the cells were washed once with a DPBS 1X solution (PBS 1X + $CaCl_2$ (0.9 mM) and $MgCl_2$ (0.9 mM)), then 200 µl of the MNPs solution were added to each well and were incubated for 1 and 3 hours. Once finished the incubation, the cells were washed 3 times with DPBS 1X solution. Then, 100 µl of paraformaldehyde 4% were added to each well and the multi-well plate was incubated during 20 minutes at 4 °C in order to fix the cells. After this time two washes were performed with DPBS 1X solution. The nucleus was stained incubating the cells with 200 µl of a previous prepared DAPI solution (1 µg/ml) for 10 minutes at room temperature. Two final washes were performed with DPBS 1X solution and finally to protect the sample, a cover slide was fixed over the chamber.

Fluorescence Microscopy

Cells were observed in a fluorescence microscope Nikon Eclipse Ti, using the following filters and acquisition parameters:

Table 1: Description of the parameters adjusted for each light filter.

Filter	Gain (s)	Exposure time (ms)
Brightfield	5	3.4
DAPI	5	8
TRITC	1.9	700

Results and Discussion

E-cadherin fragments (EC1-EC2) expression and purification

The E-cadherin WT fragments (EC1-EC2) were expressed and purified following the procedures explained in materials and methods. Once obtained, the protein fragments were attached by their His-tags on the surface of agarose microbeads which contains NTA-Ni^{2+} complexes. When the protein was eluted from the microbeads, the protein/beads ratio was determined as around 1.5 mg of protein per ml of beads.

The correct protein folding was evaluated by mixing the eluted E-cadherin fragments with trypsin in presence or absence of Ca^{2+} ions. When Ca^{2+} ions are present, some changes in the conformation occur and trypsin cannot cleave the correctly folded E-cadherin fragments. On the contrary, in the absence of Ca^{2+} ions the trypsin-mediated cleavage can occurs. In Figure 3 we can observe an SDS-PAGE gel containing the protein without any treatment and treated with trypsin in presence of Ca^{2+} ions or EDTA, a chelating agent that removes the Ca^{2+} from the media. In this gel the correct protein folding was confirmed due to the presence of a common band between the protein control and the treatment done in presence of Ca^{2+} ions (Figure 4, lanes 1-2). In addition, the single band obtained, reflected that the protein had a high purity. When the protein was treated with trypsin and EDTA, several bands located at different heights were observed, reflecting the protein cleavage (Figure 4, lane 3).

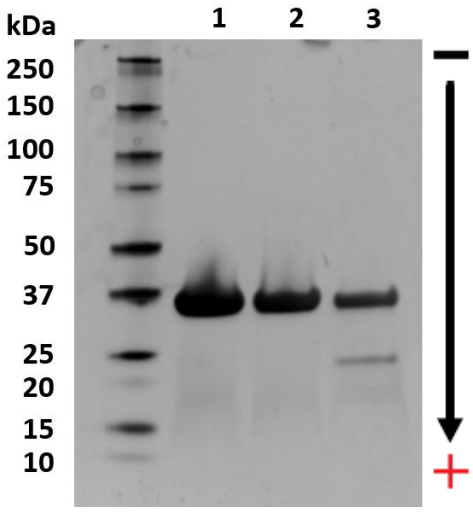

Figure 4: SDS-PAGE of the protein after trypsin sensitivity assay. **1:** Untreated E-cadherin fragments. **2:** E-cadherin fragments treated with trypsin in the presence of Ca^{2+} ions. **3:** E-cadherin fragments treated with trypsin in the absence of Ca^{2+} ions.

Water transfer of hydrophobic MNPs

The iron oxide MNPs with an average size of 12 nm used for this work were synthesized by the PhD student Eduardo Moreno by thermal decomposition method.[22] These MNPs were coated with oleic - acid and resuspended in an organic solvent (hexane). In order to use the MNPs in biological applications, the first step was to obtain water-stable MNPs (MNPs@PMAO-TAMRA), coating them with an amphiphilic polymer poly(maleic anhydride-*alt*-1-octadecene) (PMAO), modified with a fluorescent dye tetramethylrhodamine-cadaverine (TAMRA) that later facilitates the detection by fluorescence microscopy, (Figure 5).

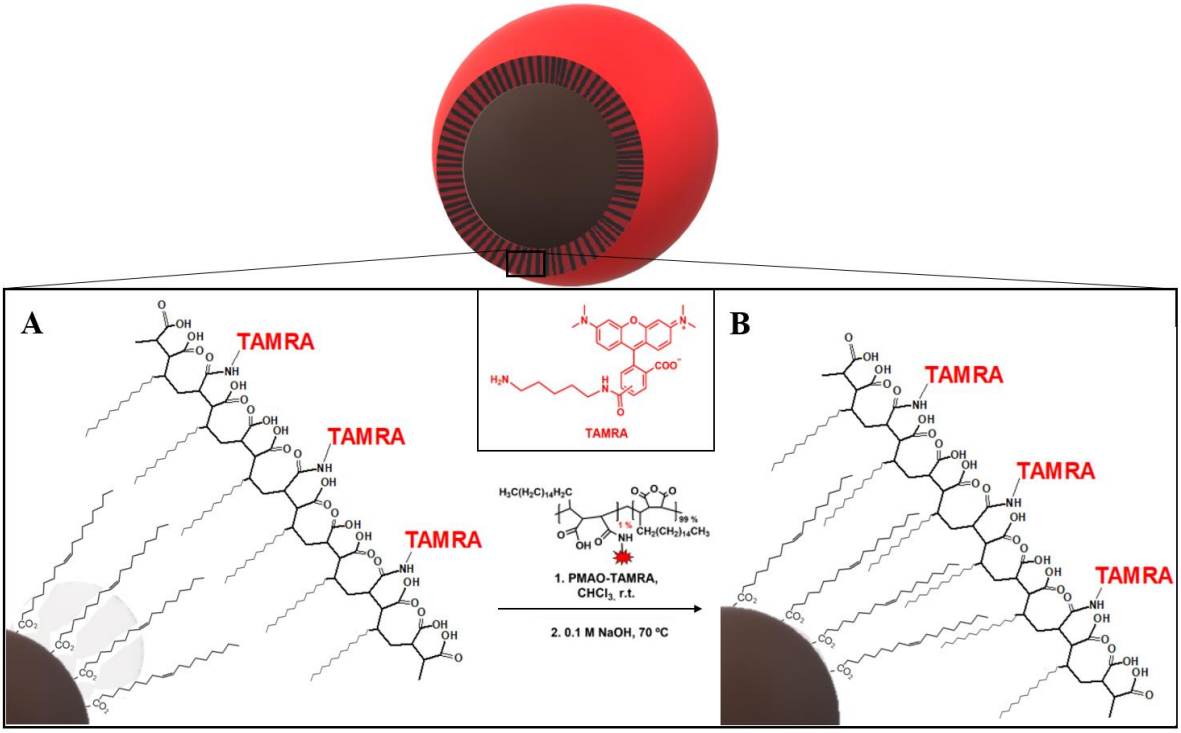

Figure 5: Scheme of the water transfer process performed of the MNPs with the PMAO-TAMRA (1%) polymer. **A:** MNPs in organic media coated with oleic acid. **B:** MNPs coated with the polymer through hydrophobic interactions. The structures of the polymer and the fluorophore are shown.

Three batches of the equivalent to 10 mg Fe in MNPs were coated with PMAO-TAMRA following the procedure explained in materials and methods. During the final washes to eliminate unreacted polymer, all the supernatants were collected and analyzed by gel electrophoresis to corroborate that the amount of unreacted polymer in the MNPs suspension diminishes after each wash. In Figure 6A we can note that the presence of fluorescence given by the PMAO-TAMRA molecules decreases after each wash and disappears completely in the fourth washing step, showing a successful elimination of the unbound polymer in the three batches.

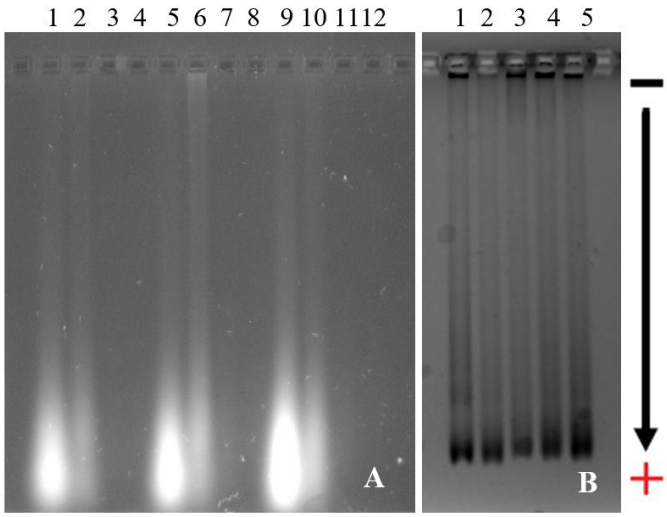

Figure 6: A: Agarose gel 1% (m/v), supernatants collected from the washing steps of water-transferred MNPs. **A: A1, A2, A3, A4**: Washes from batch 1. **A5, A6, A7, A8**: Washes from batch 2. **A9, A10, A11, A12**: Washes from batch 3. **B:** Agarose gel 1% (m/v), MNPs@PMAO@TAMRA; **B1**: Control; **B2:** batch 1; **B3, B4**: batch 2; **B5**: batch 3.

In order to test the reproducibility of the water transfer procedure, a gel electrophoresis was performed comparing the electrophoretic mobility of MNPs@PMAO-TAMRA from three different batches. In Figure 6B we can note that the three batches show a band at the same position in the agarose gel suggesting a good reproducibility of the method. Therefore, the three batches were combined in one single batch. A final quantity of 26.5 mg Fe was recovered from the three batches giving an overall yield of 88%.

Functionalization strategies

Once MNPs@PMAO-TAMRA were obtained, the next step was to functionalize them with E-cadherin fragments through three different strategies with the final aim to obtain MNPs able to attach to cell membranes in a specific and stable manner. The strategies consisted on the functionalization of the MNPs functionalization with three molecules: PEG chains, NTA-Cu^{2+} complexes and the E-cadherin protein fragments (EC1-EC2). These three molecules were functionalized in different orders as described in Table 2, always maintaining as the last step the functionalization with the protein. The two first strategies consisted on alternating the functionalization order between PEG and NTA-Cu^{2+} molecules, originating the P+N strategy (first PEG, second NTA-Cu^{2+}) and the N+P strategy (first NTA-Cu^{2+}, second PEG). The last strategy consisted on carrying out a single reaction in a one-pot fashion, adding at the same time the PEG and NTA-Cu^{2+} molecules and was designed as 1-Pot strategy.

Table 2: Description of the steps required for each functionalization strategy, starting from the water stable nanoparticles, MNPs@PMAO-TAMRA.

Strategy		Functionalization steps	
		Step 1	**Step 2**
P+N	**750**	PEG750	NTA-Cu^{2+}
	5000	PEG5000	NTA-Cu^{2+}
N+P	**750**	NTA-Cu^{2+}	PEG750
	5000	NTA-Cu^{2+}	PEG5000
1-Pot	**750**	PEG750+ NTA-Cu^{2+}	
	5000	PEG5000+ NTA-Cu^{2+}	

For each strategy (Table 2), the MNPs were grafted with two different PEG chains (molecular weights: 750 or 5000 Da), which were used in order to passivate the MNPs surface and avoid non-specific interactions during the experiments with cells. On the other hand, as the NTA-Cu^{2+} complexes can react by a highly specific non-covalent interaction with protein His-tags, these were functionalized on the MNPs surface to serve as linker agent between the MNPs and the His-tag present in the E-cadherin fragments. The protocols used in each step were described in materials and methods and were maintained between the three different strategies.

To functionalize the MNPs, with either of both PEG chains or NTA-Cu^{2+} molecules, EDC chemistry was used. The EDC molecule is a water-soluble carbodiimide that promotes a crosslinker reaction which activates the carboxyl groups present on the MNPs surface for a spontaneous reaction with primary amines. Both PEG and NTA-Cu^{2+} molecules end with a primary amine, which enabled the reaction to occur (see Figure 7 for an example of the functionalization using PEG5000) The yields obtained from the three strategies were never lower than 77% and none of the samples did show apparent aggregation (Annex A).

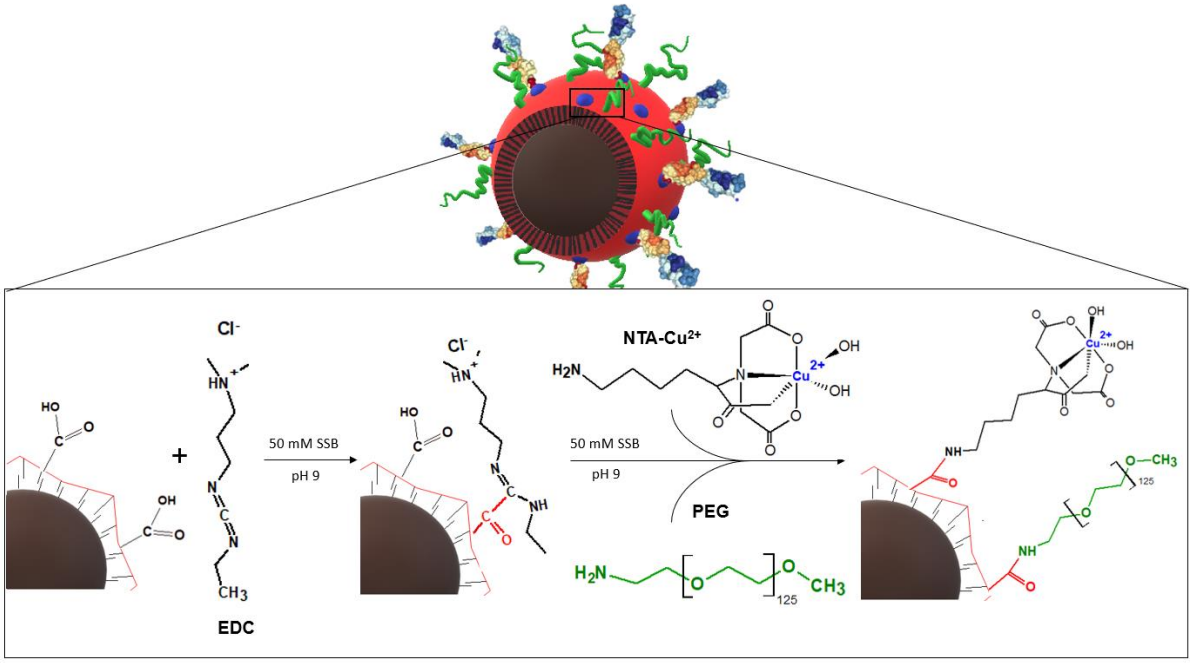

Figure 7: Scheme of the MNPs functionalization with PEG5000 and NTA. In red the PMAO-TAMRA polymer shell, showing the carboxyl groups that can be activated by the carbodiimide, reacting afterwards with the primary amines of the PEG (in green) and NTA-Cu^{2+} (in black).

In the three strategies, after each functionalization step a gel electrophoresis was performed to evaluate if a difference in the electrophoretic mobility of the MNPs appears. Thus, given the changes in size and charge of the functionalized MNPs, an electrophoretic mobility variation can be used as a first evaluation to check if a functionalization was successful. It is important to know that in the limit where the MNPs are smaller than the gel pores, the gel enables separations that varies with the nanoparticle architecture, e.g. depending on the size and charge. However, in gels where the pore and particles sizes are comparable, hydrodynamic interaction hinders the mobility mainly according to particle size.

Once completed the three strategies, all the functionalized MNPs including MNPs@PMAO-TAMRA were analyzed by gel electrophoresis to compare their electrophoretic mobility. The resultant gel is showed in Figure 8 where we can observe bands with different positions, suggesting a successful functionalization. Bands A and G, show MNPs@PMAO-TAMRA, band B to E show functionalizations that involved PEG750 chains and band H to K those that involved PEG5000 chains.

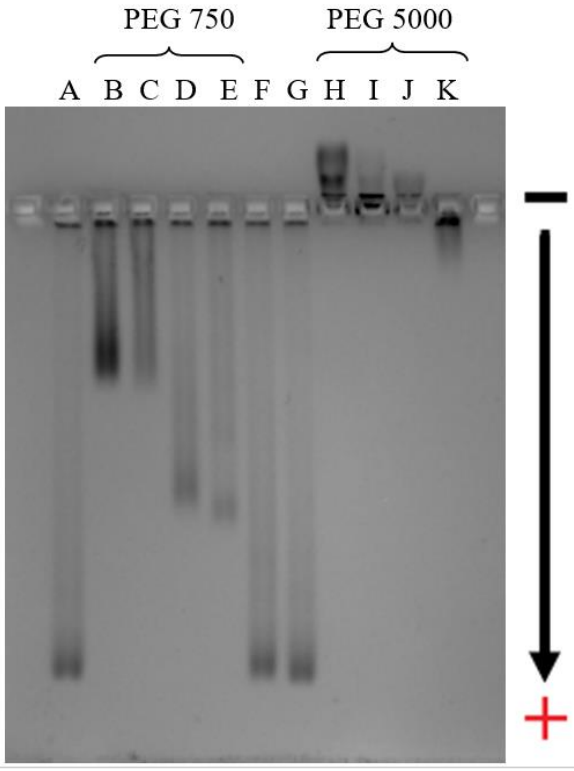

Figure 8: Agarose gel 2% (m/v) electrophoresis of the MNPs functionalized with P+N, N+P and 1-Pot strategies. **A, G**: MNPs@PMAO-TAMRA. **B:** P+N750, step 1. **C:** P+N750, step 2. **D:** N+P750, step 2. **E:** 1-Pot750. **F:** N+P750, step 1. **H:** P+N5000, step1. **I:** P+N5000, step 2. **J:** N+P5000, step 2. **K:** 1-Pot5000.

From Figure 8 it can be seen that the MNPs functionalized with PEG750 (bands B to E) had a higher electrophoretic mobility compared with those grafted with PEG5000 (bands H to K). This suggest that under the same functionalization conditions, the larger PEGs could adopt a conformation that increases the MNPs size limiting their mobility. The MNPs mobility was mainly affected by the PEG molecules (band B), whilst the solely addition of NTA-Cu^{2+} complexes practically showed no effect (band F). This suggested that the mobility was mainly dictated by the MNPs sizes instead of the charge, because in spite of the NTA-Cu^{2+} negative charges which should affect the band position, only the PEG chains that are larger promote a change.

A lower mobility was observed for the MNPs functionalized by strategy P+N (band C) compared with the other two strategies, suggesting that by functionalizing first with PEG750 chains, the polymers are free to occupy all the activated carboxyl groups on the MNPs surface increasing the final number of grafted PEG chains. On the other hand, in strategy N+P (band D), as NTA-Cu^{2+} molecules are functionalized first, they occupy a certain quantity of free carboxyl activated groups and as consequence during the second step less PEG750 molecules are grafted on the MNPs. The lower quantity of PEG chains increases the resultant MNPs mobility compared with the P+N strategy (Figure 8).

We can note that the electrophoretic mobility of the MNPs synthesized by 1-Pot strategy (band E) is more similar to the one of those coming from strategy N+P (band D) than to the one of those coming from strategy P+N (band C) (Figure 8). This will suggest that NTA-Cu^{2+} molecules have a higher affinity or a greater diffusion rate for the activated carboxyl groups present on the MNPs surface, reacting in more quantity or faster than PEG chains. Bands from H to K (were a larger PEG was used) suggested an important increase of the MNPs size, and their diminished mobility makes their analysis by gel electrophoresis more difficult.

In order to corroborate the previous results and to demonstrate the successful of the functionalization, DLS and ζ-potential analysis were performed to obtain the hydrodynamic diameter and the surface charges of the functionalized MNPs. The results obtained showed that the MNPs@PMAO-TAMRA had a hydrodynamic diameter of 80 ± 1 nm and a ζ-potential of -48 ± 0.4 mV. The rest of the data from the functionalization strategies are showed in Table 3 and the intensity graphs obtained by DLS analysis are available in Annex B.

Table 3: Hydrodynamic diameter determined from DLS intensity curves and ζ-potential of MNPs@PMAO-TAMRA functionalized by the three strategies.

Strategy		**Functionalization Step**			
		Step 1		**Step 2**	
		Diameter (nm)	**ζ-potential (mV)**	**Diameter (nm)**	**ζ-potential (mV)**
P+N	**750**	82 ± 0.3	-19 ± 0.1	83 ± 0.6	-21 ± 1
	5000	108 ± 0.7	-2 ± 0.3	110 ± 0.5	-15 ± 0.4
N+P	**750**	76 ± 0.6	-34 ± 0.5	77 ± 0.3	-22 ± 0.2
	5000	76 ± 0.6	-34 ± 0.5	98 ± 1	-17 ± 0.5
Strategy		**Diameter (nm)**		**ζ-potential (mV)**	
1-Pot	**750**	83 ± 0		-24 ± 0.4	
	5000	99 ± 2		-15 ± 0.3	

In Table 3, we can observe that almost all the hydrodynamic diameters showed a tendency to increase after each functionalization step. Only the N+P strategy, showed a hydrodynamic diameter (76 ± 0.6) lower than MNPs@PMAO-TAMRA (80 ± 1) after functionalization with NTA-Cu^{2+}. This small variation is negligible given the small size of the NTA-Cu^{2+} molecules when compared with the MNPs starting size. A small population of aggregates was observed in the MNPs synthesized by strategies

P+N5000 and N+P5000, nevertheless, as the polydispersity indexes never overpassed 0.3, we concluded that the MNPs were not highly aggregated (Annex B).

On the other hand, from ζ-potential measurements we can note that in the three strategies, the negative charges present on the MNPs surface diminished after the first functionalization step, confirming the results from the gel electrophoresis and proving a successful functionalization either with NTA-Cu^{2+} or PEG. During the second functionalization step, the strategy N+P maintained the same pattern as neutral PEG molecules were incorporated, however, a different behavior appeared on strategy P+N, evidencing the negative charge increasing promoted by the negative functionalized NTA-Cu^{2+} complexes.

From all the previous results we can conclude that all the MNPs were successfully functionalized by the three strategies and also that were not aggregated maintaining a nanometer size acceptable to bind small receptors such as cadherins.[49] Thus, the next step was to functionalize all of them with the E-cadherin WT fragments (EC1-EC2).

Functionalization with E-cadherin WT fragments

All the MNPs were functionalized with E-cadherin WT fragments EC1-EC2 (100 µg/mg Fe). The procedure from materials and methods was followed leaving the MNPs reacts with the protein fragments in presence or absence of imidazole. The imidazole molecule is a small nitrogen-containing heterocyclic ring, which during the protein immobilization acts as a competitor against the His-tag tail for binding to the NTA-Cu^{2+} complexes. Thus, when imidazole is present the protein fragments immobilization turns much less probable, allowing us to determine if the functionalization that is taking place is mediated by the His-tag sequence, or in other words, if the protein immobilization on the MNPs surface occurs in an oriented-manner (Figure 9).

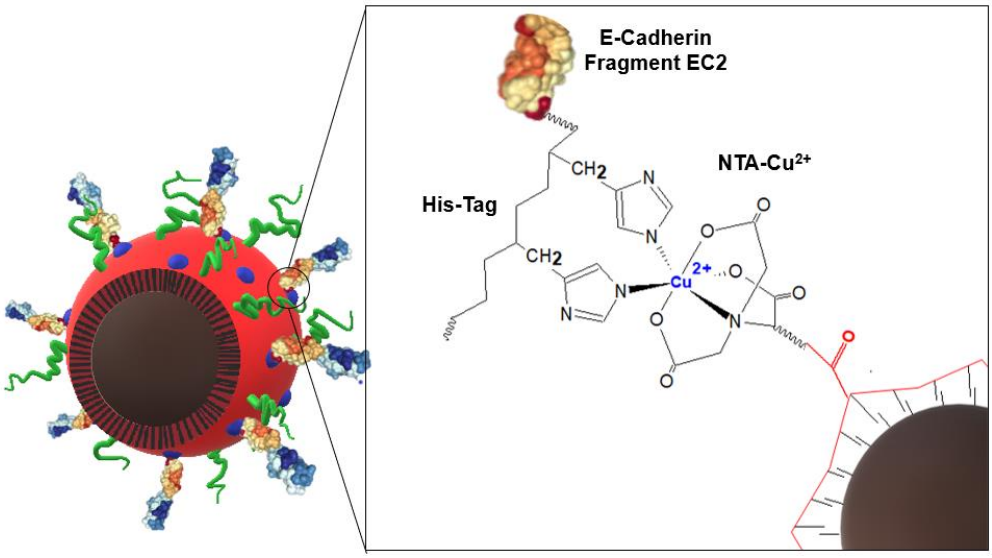

Figure 9: Scheme of the MNPs functionalization with E-cadherin protein fragments EC1-EC2 in an oriented manner.

Once the MNPs reacted with the protein fragments in presence or absence of imidazole a centrifugation step was performed, the resultant pellets were resuspended in PBS 1X solution (w/o Ca, w/o Mg) and were used to evaluate the MNPs stability, first visually (Figure 10) and then using an inverted brightfield microscope at 10 and 20X objective magnification (Annex C). Table 4 summarizes the stability of all the conjugations performed.

Table 4: Stability of MNPs conjugated with E-cadherin WT fragments (EC1-EC2), in presence or absence of imidazole (0.25 M).

Strategy		**Aggregation**	
		Without Imidazole	**Imidazole (0.25 M)**
Controls	@PEG 750	-	-
	@PEG 5000	+	+
	@NTA-Cu^{2+}	+++	-
P+N	**750**	-	-
	5000	++	++
N+P	**750**	+++	+
	5000	+	+
1+Pot	**750**	+++	-
	5000	+	+

-: No visual aggregation; +: Small aggregates; ++: Highly aggregated: +++: Difficult/impossible to resuspend.

We could observe after the protein immobilization, that some of the MNPs aggregated more easily. This stability change can be explained by the fact that, if there are proteins immobilized on the MNPs surface, they could affect the MNP charge and stability, promoting their aggregation. In this sense, we correlated the existence of a functionalization with the presence of MNPs aggregation.

From the controls present in Table 4, we can note that the stability of the MNPs functionalized only with PEG molecules was not affected by imidazole molecules (Figure 10A). As there was not change in stability in the presence or absence of imidazole, this behavior suggested that the proteins could not be immobilized on the MNPs surface, supporting the idea that a good passivation was accomplished. On the contrary, the control MNPs modified only with NTA-Cu^{2+} complexes, showed a clear difference when imidazole was added. In presence of imidazole these MNPs showed a high stability as cadherin fragments could not be attached, however, when imidazole was not present the aggregation was higher due to cadherin functionalization (Figure 10B). These three controls are in concordance with the correlation described between the functionalization and aggregation, because in this scenario the only MNPs that could result aggregated, are those in which the proteins are immobilized in the absence of imidazole, as occurred in our results.

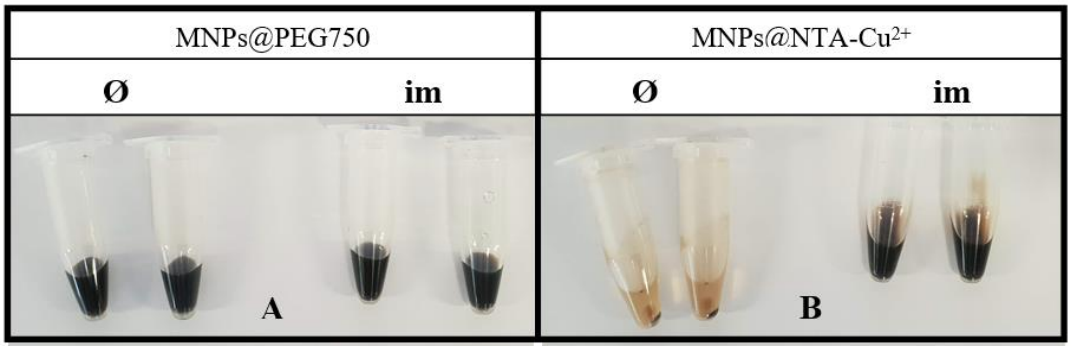

Figure 10: A: MNPs functionalized with E-cadherin WT protein fragments EC1-EC2 (100 µg/mg Fe) in the absence (**Ø**) or presence of imidazole (0.25 M) (**im**). **A:** MNPs@PEG750; **B:** MNPs@NTA-Cu^{2+}.

On the other hand, in strategy P+N, there was not difference in the MNPs stability after the functionalization in presence or absence of imidazole (Table 4). This can be explained by the fact that in this strategy the PEG chains were added in the first place, and, as was claimed before this would cause that less NTA-Cu^{2+} molecules to be functionalized. Then, as are less NTA-Cu^{2+} complexes present on the MNPs surface, the quantity of E-cadherin WT fragments immobilized should be lower and at the end, with or without imidazole there was not enough quantity of immobilized proteins to alter the MNPs stability, supporting this hypothesis.

Following the same thinking, as the NTA-Cu^{2+} complexes are functionalized in more quantity by strategies N+P and 1-Pot, more proteins should be immobilized if imidazole is not present. In Table 4 we can observe a clear difference in the stability in presence or absence of imidazole in the case of the MNPs functionalized by N+P750 or 1-Pot750. Here, the presence of imidazole maintained the MNPs stability as cadherins could not be attached, whilst, when imidazole was absent, a high aggregation occurred, demonstrating an oriented protein immobilization mediated by the His-tag sequence. On the other hand, the MNPs functionalized by the N+P5000 and 1-Pot5000 strategies did not show differences in the stability due to the presence of imidazole. This could mean that the coating with larger PEG chains could help to maintain a higher steric stability after the functionalization or that the immobilization is not taking place because PEG chains, due to their length, are hiding the NTA-Cu^{2+} complexes.

For a better understanding of the stability results and in order to contrast this information with the quantity of protein immobilized, the supernatants from the functionalization with E-cadherin WT fragments were collected and analyzed by the dot-blot immunoassay, comparing with the initial protein stock solution. The semiquantitative results obtained are showed in the Figure 11.

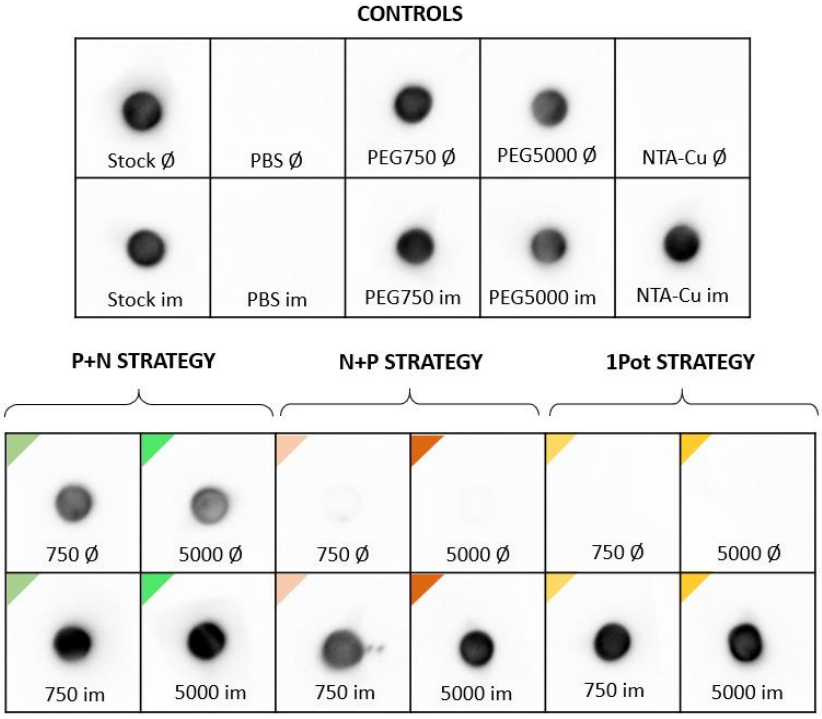

Figure 11: Dot-blot of the protein present in the supernatants recovered from the MNPs functionalization with E-cadherin WT fragments. **Ø:** Functionalizations without imidazole; **im:** Functionalizations with imidazole (0.25 M). **Stock:** Protein stock solution; **PEG750:** MNPs@PMAO-TAMRA@PEG750; **PEG5000:** MNPs@PMAO-TAMRA@PEG5000; **NTA-Cu**: MNPs@PMAO-TAMRA@NTA-Cu^{2+}. **750, 5000:** Functionalizations using MNPs that contains a coat of PEG750 or PEG5000 chains respectively.

In Figure 11, different controls were included (upper row). We can observe that the presence of imidazole does not affect the signal given by the initial protein stock solution (Stock Ø, im) used to functionalize the MNPs and that the PBS solution does not give any signal (PBS Ø, im), as expected. The supernatant recovered from MNPs@PEG750, gave the same signal in presence or absence of imidazole (PEG750 Ø, im), which was also similar to the signal from the protein stock solution. The same occurred with MNPs@PEG5000 (PEG5000 Ø, im), suggesting that none or low quantity of E-cadherin WT fragments were bound non-specifically to these MNPs due to the passivation generated by PEG molecules, in concordance with the stability showed in Table 4.

On the other hand, the supernatants collected from the MNPs@NTA-Cu^{2+}, showed a total absence of intensity in the signal corresponding to the treatment without imidazole, whilst, the signal resultant from the treatment with imidazole had an intensity similar to the protein stock solution. This difference is also consistent with the results obtained from the stability observations, demonstrating that the E-cadherin WT fragments were immobilized in an oriented manner on the MNPs surface when the competitor imidazole was not present, whilst, the immobilization did not occur when imidazole was added.

The MNPs synthesized by N+P and 1-Pot strategies were those able to immobilize more quantity of E-cadherin WT fragments on their surfaces (Figure 11, lower rows). This confirms that, as previously suggested, more NTA-Cu^{2+} complexes were present on the MNPs surface, thus promoting a greater immobilization of E-cadherin WT fragments in an oriented manner. The MNPs functionalized by P+N strategy bound fewer E-cadherin fragments, as less NTA-Cu^{2+} molecules were present on the surface.

Taking into account these results, the MNPs obtained by strategies N+P and 1-Pot showed the highest stability and were able to immobilize higher amounts of proteins. Nevertheless, because of the timesaving and the easiness of using a one-pot reaction, we decided to continue working only with the 1-Pot strategy, conserving the grafting with both PEG chains.

The next step was to find a maximum E-cadherin concentration that did not lead to the aggregation of the MNPs due to surface changes. Increasing concentrations of E-cadherin WT fragments, ranging from 1 to 250 µg protein/ mg Fe, were used, Figure 12 shows the results obtained from the cadherin-functionalized MNPs synthesized by 1-Pot750 and 1-Pot5000 strategies.

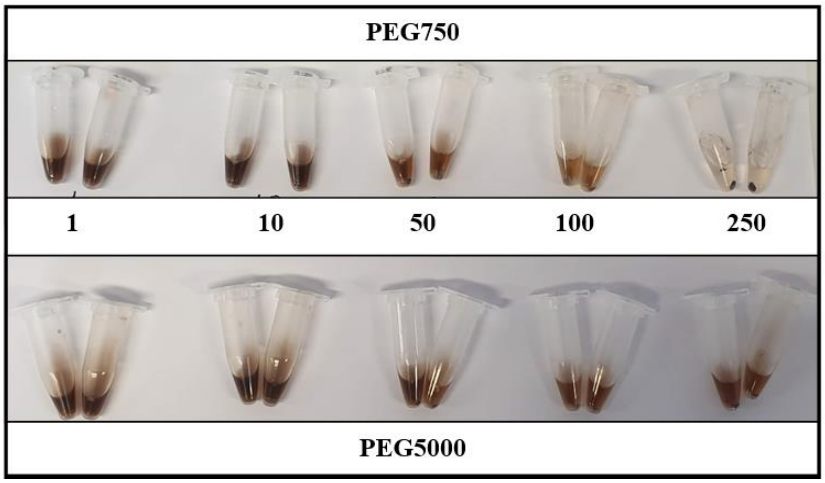

Figure 12: MNPs obtained by strategies 1-Pot750 or 1-Pot5000 and functionalized with five E-cadherin WT fragments concentrations (1, 10, 50, 100, 250 µg protein/ mg Fe).

The resultant MNPs showed that the higher the E-cadherin WT fragments concentration is, the lower is the MNPs stability in PBS 1X (w/o Ca and w/o Mg). Furthermore, it was observed that as the concentrations of E-cadherin WT fragments increased, the MNPs obtained by strategy 1-Pot5000 showed a higher stability when compared with strategy 1-Pot750 (Figure 12); this was expected, given the greater passivation reached by using larger PEG chains.

After a short sonication, the MNPs synthesized by strategy 1-Pot750 were well resuspended only when using up to 50 µg of protein/mg Fe, whilst, the MNPs from strategy 1-Pot5000 were completely resuspended even using 100 µg of protein/mg Fe. Nevertheless, the MNPs were harder to resuspend with this last concentration.

The next step was to semiquantitatively evaluate the amount of protein immobilized on the MNPs using these five protein concentrations. As explained before, a dot-blot of the supernatants recovered after the functionalization process was performed. Figure 13 shows the results obtained.

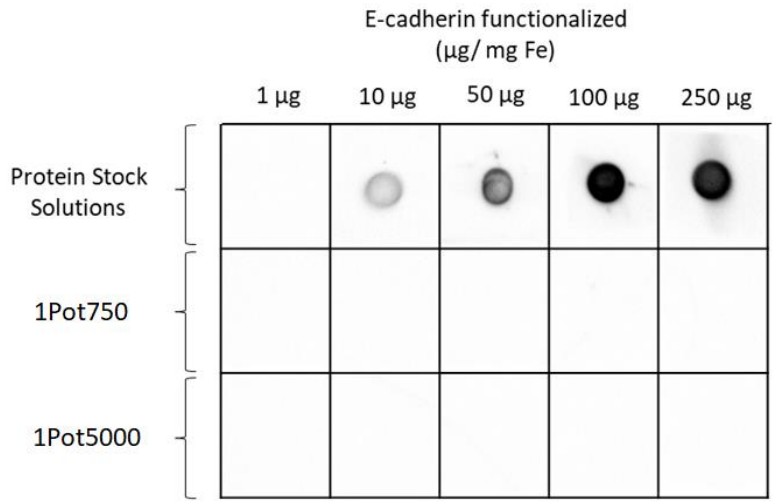

Figure 13: Dot-blot showing the presence of protein in the supernatants recovered after MNPs functionalization with five concentrations of E-cadherin WT fragments (1, 10, 50, 100, 250 µg protein/ mg Fe). **1Pot750:** MNPs obtained by 1-Pot strategy using PEG750**; 1Pot5000:** MNPs obtained by 1-Pot strategy using PEG5000**.**

In Figure 13, we can observe that for all the protein concentrations tested, a total absence of signal intensities appears, indicating that practically all or at least a great part of the protein added was immobilized onto the MNPs surface. This could be explained by a high number of NTA-Cu^{2+} complexes present on the MNPs. As in all cases the protein immobilization was high, we selected the condition that showed a better stability. Thus, 50 µg of protein/mg Fe was chosen as the best protein concentration to be immobilized on the MNPs surface in an oriented manner.

Aside from the MNPs functionalized with the E-cadherin WT fragments, MNPs functionalized with the W2A mutant fragments were also synthesized. This functionalization was performed by using the same 1-Pot750 or 1-Pot5000 strategies, as well as, the same protein concentration (50 µg protein/ mg Fe) obtaining similar results.

Interaction of the MNPs with cell membranes

Once functionalized the MNPs, the next step was to immobilize them on cell membranes. To achieve this goal, was also important to keep in mind the cell type and variety of cadherins expressed on the cell membranes, which will dictate the specificity of the interaction. For this reason, to evaluate the MNPs immobilization we used two different cell-lines: an epithelial cell line (Madin-Darby Canine Kidney, MDCK) and a fibroblast-like cell line (BALB/c3T3), expressing and lacking E-cadherin proteins on their cell membrane, respectively.[50]

Before attaching the MNPs to the cell membrane, we conducted a stability test to know if the MNPs aggregated in cell culture media. For that, we mixed the MNPs with DMEM with and without FBS and changes in the stability were observed under the inverted microscope. The results obtained are showed in Figure 14.

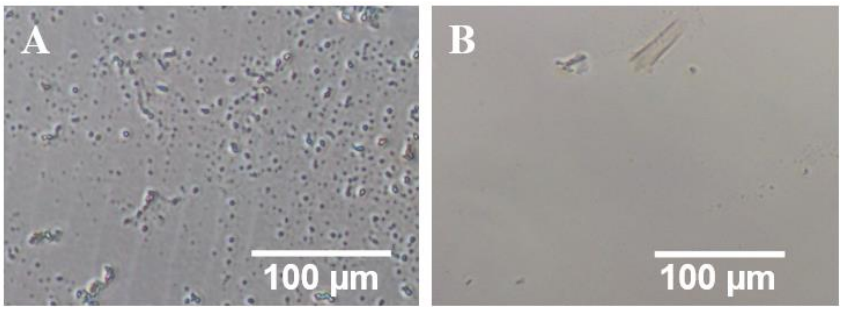

Figure 14: MNPs obtained by strategy 1-Pot5000 incubated during 15 minutes with: **A:** complete DMEM medium (10X). **B:** DMEM without FBS (10X).

We observed that the MNPs tended to form more aggregates in the medium containing FBS (Figure 14A), whilst, in DMEM medium without FBS the MNPs showed less aggregation (Figure 14B). These results suggest that some components of the FBS interact with the MNPs in a non-specific manner, promoting the aggregation. This can lead to a change of the biological entity of the MNPs, that can ultimately hide the E-cadherin fragments present on their surface. To avoid this problem and minimize non-specific interaction with the cells, we used DMEM without FBS during the incubation time with the MNPs.

The immobilization was assessed using MNPs prepared by 1-Pot750 or 1-Pot5000 strategies and functionalized with E-cadherin fragments WT or W2A mutant fragments. The W2A fragments were used to test their influence on the interaction, since the Trp2 presence is crucial for the homophilic interaction process and its replacement could show a different immobilization pattern. For instance, a previous work from our group using microbeads functionalized with W2A fragments has showed that these particles can interact with the cells but to a lesser extent than those functionalized with WT fragments. Further, once the microparticles are immobilized on the cells, they do not induce membrane movements, and therefore the microparticles are retained for longer periods of time in the membrane (Moros, M., et al., unpublished results).

Once incubated with the MNPs for one or three hours, the cells were fixed, their nuclei stained with DAPI and they were observed by fluorescence microscopy using the acquisition parameters detailed in materials and methods. Figure 15 shows the images captured using MDCK cells incubated with the MNPs obtained by strategy 1-Pot750, whilst, Figure 16 shows the cells incubated with the MNPs

obtained by strategy 1-Pot5000. In both figures, MNPs bearing PEG but without protein fragments were used as a control and the pictures were taken after one and three hours of incubation.

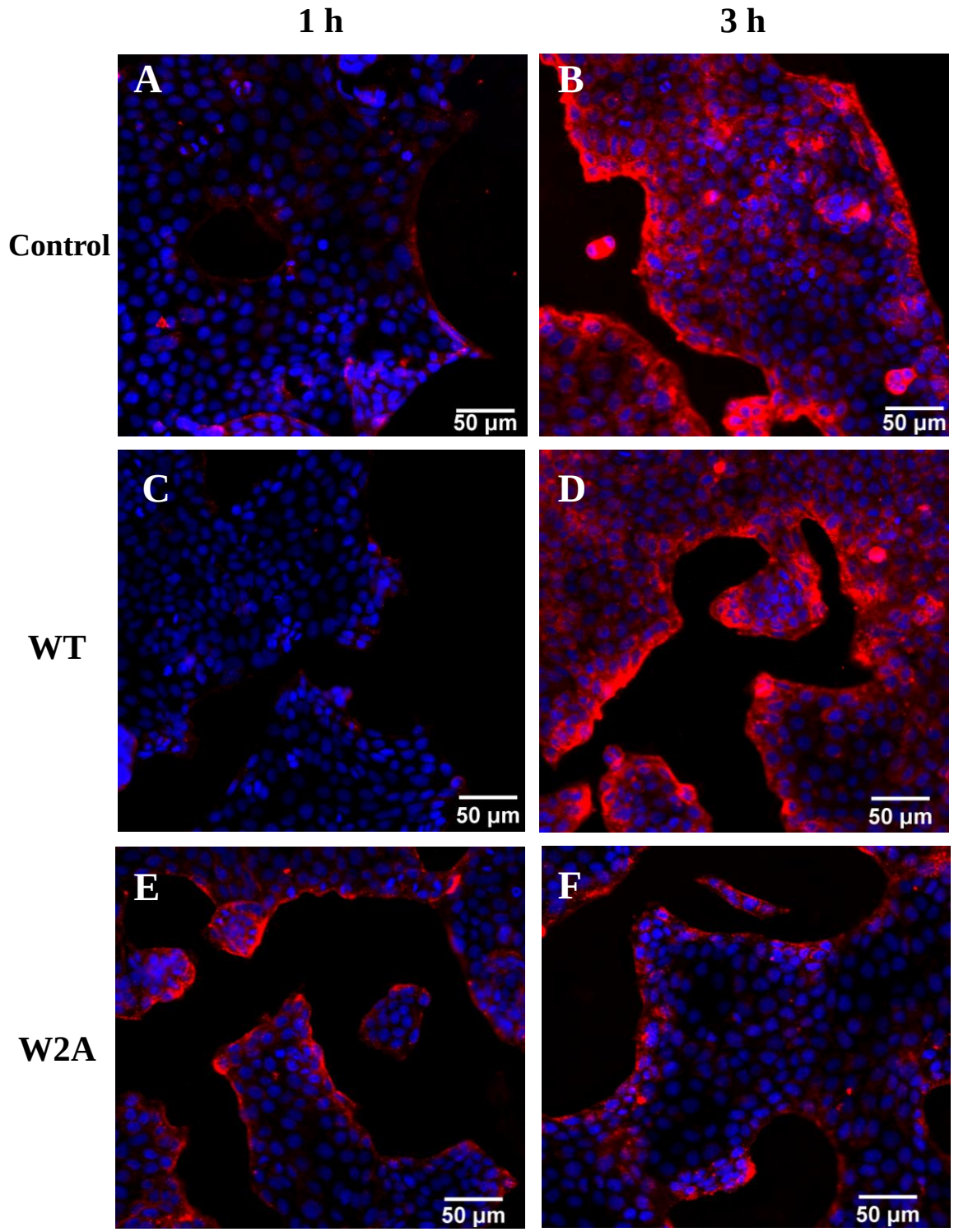

Figure: 15: MDCK cells, **A:** MNPs 1-Pot750 without E-cadherin fragments 1h. **B:** MNPs 1-Pot750 without E-cadherin fragments, 3h. **C:** MNPs 1-Pot750 + WT fragments, 1h. **D:** MNPs 1-Pot750 + WT fragments, 3h. **E:** MNPs 1-Pot750 + W2A fragments, 1h, **F:** MNPs 1-Pot750 + W2A fragments, 3h. (**Scale bar**: 50 µm).

In Figure 15, control MNPs (Figure 15A, 15B), as well as, the MNPs immobilized by WT fragments (Figure 15C, 15D) showed that as the incubation time increased from one to three hours more MNPs were detected in the cells. This behavior suggests that when the incubation time is longer, the probability of MNPs interacting with the cells is higher. This signal from the MNPs can arise from MNPs immobilized on the cell membranes or internalized by the cells; the fact that control MNPs gave a similar signal than WT-functionalized MNPs suggests a non-specific interaction. Further, interaction between cadherins should be quickly promoted, while in this case after one hour of incubation almost no signal can be found. To understand where the signal is coming from, further confocal microscopy or internalization studies are needed.

On the other hand, the MNPs immobilized by W2A fragments (Figure 15E, 15F) showed a greater signal after one hour of incubation, suggesting a faster and more specific interaction with the cells. Furthermore, a similar intensity pattern was obtained after 1 or 3 hours of incubation, which can be due to a lower interaction or internalization, similar to the results obtained with the microbeads. This will mean that the W2A mutation affects the protein-protein interactions and, as consequence, does not trigger the same responses in the cells, which could also include differences in the internalization process.

The results obtained by using 1-Pot5000 strategy (Figure 16) instead of 1-Pot750 strategy (Figure 15), revealed an important variation regarding the interactions with the cells. The coating with a larger PEG diminished the intensity of all the treatments evaluated (Figure 16), confirming a better passivation of the MNPs, consequently, less MNPs were able to interact with the cells in a non-specific way.

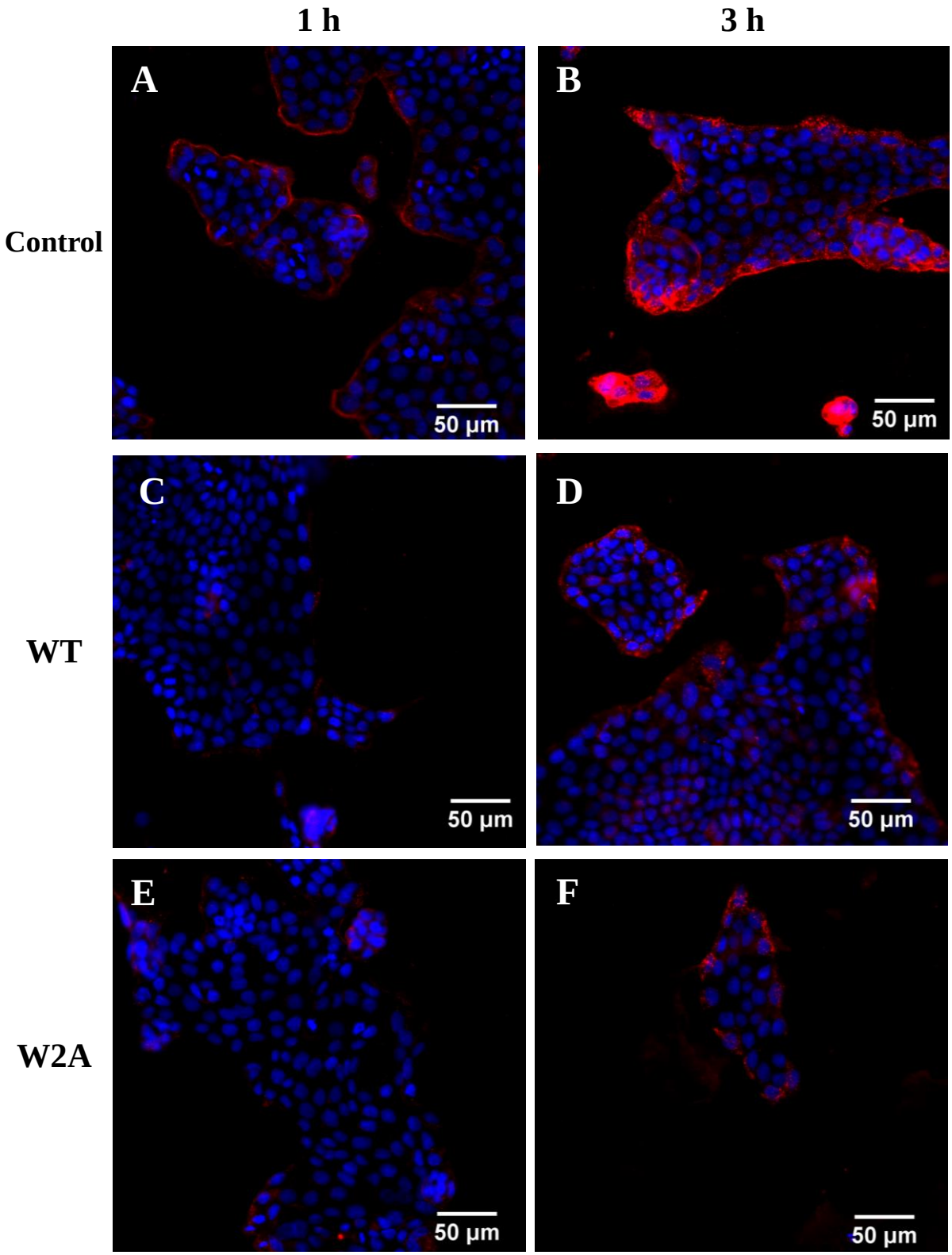

Figure 16: MDCK cells, **A:** MNPs 1-Pot5000 without E-cadherin fragments 1h. **B:** MNPs 1-Pot5000 without E-cadherin fragments, 3h. **C:** MNPs 1-Pot5000 + WT fragments, 1h. **D:** MNPs 1-Pot5000 + WT fragments, 3h. **E:** MNPs 1-Pot5000 + W2A fragments, 1h **F:** MNPs 1-Pot5000 + W2A fragments, 3h. (**Scale bar**: 50 µm)

In Figure 16, we can observe that when using PEG5000 the intensity given by the MNPs increased with the incubation time in all cases. However, the intensity given by the MNPs immobilized by WT fragments after one or three hours (Figure 16C, 16D), was lower compared with the control MNPs (Figure 16A, 16B). This suggests that a larger PEG could be diminishing non-specific interactions, improving therefore the specific interaction between the WT fragments and the cellular cadherins.

Unlike the MNPs functionalize by strategy 1-Pot750, in this case the larger PEG promoted that the MNPs functionalized with WT fragments (Figure 16C, 16D) behaved more similarly to the MNPs functionalized with W2A fragments (Figure 16E, 16F). Thus, both showed a low intensity even after three hours, suggesting a lower interaction with the cells that could mean more specific immobilization. Additional confocal microscopy studies and signal quantification will be performed in future works to test this hypothesis, as the interaction between cadherins should occur in a faster way.

To obtain more information about the specific interaction of the MNPs with E-cadherins present on cells, the same experiments carried out with MDCK cells were performed using BALB/c3T3cells that lack E-cadherin. As before, MNPs bearing PEG but without protein fragments were used as a control and the images were taken after three hours of incubation. In Figure 17 the results obtained are showed.

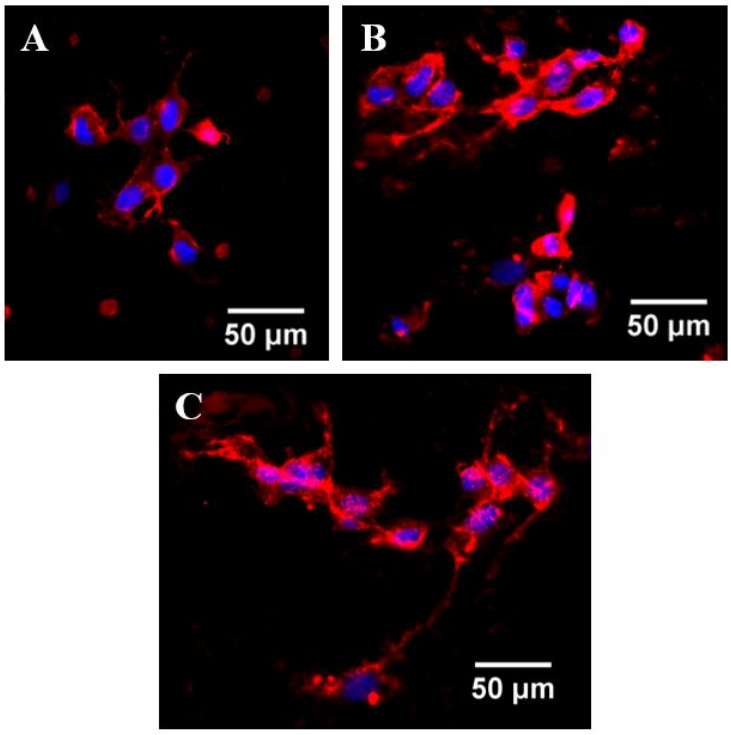

Figure 17: BALB/c3T3 cells, **A:** MNPs 1-Pot5000 + WT fragments, 3h. **B:** MNPs 1-Pot750 without E-cadherin fragments, 3h. **C:** MNPs 1-Pot5000 + W2A fragments, 3h. (**Scale bar**: 50 µm)

All the MNPs evaluated after one or three hours of incubation showed similar fluorescence intensities and appear all over the cell (Figure 17, results showed only for 3 h of incubation). Since BALB/c3T3 cells do not express E-cadherin proteins, this behavior is indicative of non-specific interactions with the cell membranes. Only the MNPs synthesized by 1-Pot5000 strategy (Figure 17A) showed a slightly variation on the signal intensities; however, this intensity decrease could be a consequence of the MNPs surface passivation mediated by the larger PEG chains.

The interactions observed between the MNPs and BALB/c3T3 cells did not show differences between all the different MNPs tested (Figure 17). On the other hand, the interactions between the MNPs and the MDCK cells in which E-cadherin protein is expressed, showed clear differences between the different MNPs. These differences when using diverse cell lines are an important first step to hypothesize that MNPs functionalized with cadherin fragments can be selectively immobilized on the surface of living cells. Future works will need to be performed in order to decipher the location of the MNPs, and to obtain specific immobilization for longer period of times.

Conclusions

After obtaining water-stable MNPs, three functionalization strategies (P+N, N+P and 1-Pot), were tested to introduce passivating molecules and NTA-Cu^{2+} complexes on the MNPs surface. In all cases both molecules were successfully functionalized, although with different yields depending on the order of performing the reaction. The 1-Pot strategy, where MNPs coated by PMAO-TAMRA were functionalized with PEG750 or PEG5000 and NTA-Cu^{2+} complexes at the same time was selected as the most suitable. This strategy allowed us to obtain MNPs with overall average yields of 77%, which showed low aggregation in PBS solution, using a one-pot reaction, making it a fast more economic and reproducible method.

E-cadherin protein fragments WT or W2A, were successfully immobilized on the MNPs surface. Since the number of NTA-Cu^{2+} complexes on the MNPs surface was higher than with other strategies, large quantity of protein could be attached in an oriented manner on their surface. Based on stability assays, we selected 50 µg protein/ mg Fe as the optimal concentration that allowed us to obtain MNPs with a low aggregation in cell culture medium, making them suitable for cell culture experiments.

The interaction of the MNPs with MDCK cells, allowed us to observe that the MNPs functionalized following the 1-Pot750 strategy showed a higher interaction with the cells compared with those functionalized by 1-Pot5000 strategy, suggesting that larger PEG chains passivated better the MNPs surface, limiting non-specific MNPs-cells interaction.

The functionalization with the mutated E-cadherin fragments (W2A), diminished the interaction with MDCK cells in all the cases, suggesting that the W2A mutation affect the MNPs-cells interactions and, as consequence, do not trigger the same accumulation in the cells. Nevertheless, more studies are required to understand this mechanism of interaction and also to test the specificity of the MNPs with the E-cadherins present on the cell membranes.

This work represents a first attempt towards the development of an immobilization strategy mediated by cadherin-cadherin interactions with the desired characteristics for perform hyperthermia studies on living cell membranes. The different behaviors observed during the MNPs-cells interaction were highly dependent on the composition of the MNPs surface. This suggest that optimizing parameters such as the quantity of protein immobilized on the MNPs surface, the length and quantity of the PEG chains grafted, the size of the MNPs or others like the time of interaction with cells, or the concentration of the MNPs used, could help to adjust the specificity and stability of the MNPs immobilization on the membranes of E-cadherin expressing cells.

Future Perspectives

In order to understand better the mechanism by which the MNPs are being functionalized using the 1-Pot strategy, it could be useful to test different ratios of NTA-Cu^{2+}:PEG molecules and to correlate the number of PEG molecules with the electrophoretic mobility.

In future works, it is recommendable to test different MNPs concentrations in order to evaluate the interaction with cell membranes, as a suitable concentration could help to differentiate the most promising MNPs for the hyperthermia studies.

Finally, time lapse and confocal microscopy analysis could be carried out in order to obtain more information about the ultimate intracellular localization of the MNPs and about the time frame in which the MNPs remain attached to the cell membrane.

Bibliography

1. Conde, J., Dias, JT., Grazú, V., Moros, M., Baptista, PV., and de la Fuente, JM. (2014). Revisiting 30 years of biofunctionalization and surface chemistry of inorganic nanoparticles for nanomedicine. *Frontiers in Chemistry*, *2*(48).
2. Zhang, L., Gu, FX., Chan, JM., Wang, AZ., Langer, RS., Farokhzad, OC. (2008). Nanoparticles in Medicine: Therapeutic Applications and Developments. *Clinical Pharmacology & Therapeutics*, *83*(5), 761.
3. Singh, R., and Naiwa, HS. (2011). Medical Applications of Nanoparticles in Biological Imaging, Cell Labeling, Antimicrobial Agents, and Anticancer Nanodrugs. *Journal of Biomedical Nanotechnology*, *7*4(4), 489.
4. Kudr, J., Haddad, Y., Richtera, L., Heger, Z., Cernak, M., Adam, V., & Zitka, O. (2017). Magnetic Nanoparticles: From Design and Synthesis to Real World Applications. *Nanomaterials (Basel, Switzerland)*, *7*(9), 243.
5. Nagamune, T. (2017). Biomolecular engineering for nanobio/bionanotechnology. *Nano convergence*, *4*(1), 9.
6. Guerrini, L., Alvarez-Puebla, R. & Pazos-Perez, N. (2018). Surface Modifications of Nanoparticles for Stability in Biological Fluids. *Materials*, *11*, 1154.
7. Stepien, G. (2017). Interactions of Magnetic Nanoparticles with Proteins, Cells and living organisms for Magnetic Hyperthermia Applications (PhD thesis). Universidad de Zaragoza, Zaragoza, España.
8. Ramos, A. P., Cruz, M., Tovani, C. B., & Ciancaglini, P. (2017). Biomedical applications of nanotechnology. *Biophysical reviews*, *9*(2), 79.
9. Nguyen, D., and Kim, KS. (2014). Functionalization of magnetic nanoparticles for biomedical applications. Korean J. Chem. Eng, 31(8), 1289.
10. Moros, M. (2012). Síntesis de Gliconanopartículas Magnéticas para Aplicaciones Biomédicas (PhD thesis). Universidad de Zaragoza, Zaragoza, España.
11. Akbarzadeh, A., Samiei, M., & Davaran, S. (2012). Magnetic nanoparticles: preparation, physical properties, and applications in biomedicine. *Nanoscale research letters*, *7*(1),144.
12. Frimpong, R., & Hilt, J. (2010). Magnetic nanoparticles in biomedicine: synthesis, functionalization and applications. *Future Medicine: Nanomedicine*, *5*(9), 1401.
13. Blanco, E., Shen, H., Ferrari, M. (2011). Principles of Nanoparticle Design for Overcoming Biological Barriers to Drug Delivery. *Nature Biotechnology*, *33*, 941.
14. Neamtu, M., Nadejde, C., Hodoroaba, V., Schneider, R., Verestiuc, L. & Panne, U. (2018). Functionalized magnetic nanoparticles: Synthesis, characterization, catalytic application and assessment of toxicity. *Scientific Reports*, *8*, 6278.
15. Moreno, E. (2018). Oriented functionalization of magnetic nanoparticles with E-cadherin. (Final Master Project). Universidad de Zaragoza, Zaragoza, España.
16. Chen, L., Chen, Ch., Wang, P. & Song, T. (2017). Mechanism of cellular effect directly induced by magnetic nanoparticles under magnetic fields. *Journal of Nanomaterials*, 1564634.
17. Huang, H.; Delikanli, S.; Zeng, H.; Ferkey, D. M.; Pralle, A. (2010). Remote Control of Ion Channels and Neurons through Magnetic-Field Heating of Nanoparticles. *Nature Nanotechnology*, 5, 602.
18. Hachani, R., Birchall, M., Lowdell, M., Kasparis, G., Tung, L., Manshian, G., Soenen, S., Gsell, W., Himmelreich, U., Gharagouzloo, C., Thanh, N. (2017). Assessing cell-nanoparticle interactions by high content imaging of biocompatible iron oxide nanoparticles as potential contrast agents for magnetic resonance imaging. *Scientific reports*, *7*(1), 7850.
19. Catalayud, B., Sanz, V., Raffa, C., Riggio, M.R., Ibarra, Goya, G. (2014). Protein adsorption onto Fe3O4 nanoparticles with opposite surface charge and its impact on cell uptake. *Biomaterial*, *35*(24), 6389.
20. Alavi, M. & Hamidi, M. (2019). Passive and active targeting in cancer therapy by liposomes and lipid nanoparticles. *Drug Metabolism and Personalized Therapy*, *34*(1).

21. Nguyen, T. (2018). Clinical Applications of Magnetic Nanoparticles: From Fabrication to Clinical Applications. *CRC Press-Taylor & Francis Group, 1,* 175.
22. Fratila, R., Navascuez, M., Idiago-López, M., Eceiza, J., Miranda, I., Aizpurua, M. & J. de la Fuente, J. Covalent immobilisation of magnetic nanoparticles on surfaces via strain-promoted azide–alkyne click chemistry. *New Journal of Chemistry, 41,* 10835.
23. Keefe, A., Supriya Pai, S. & Andrew Ellington. (2010). Aptamers as therapeutics. *Nature Reviews Drug Discovery, 9,* 537.
24. Mout, R., Moyano, D. F., Rana, S., & Rotello, V. M. (2012). Surface functionalization of nanoparticles for nanomedicine. *Chemical Society Reviews, 41*(7), 2539.
25. Wang, TH., & Lee, WC. (2003). Immobilization of proteins on magnetic nanoparticles *Biotechnological Bioprocess Engineering, 8*(263).
26. Patil, U., Adireddy, S., Jaiswal, A., Mandava, S., Lee, B., Chrisey, D. (2015). In Vitro/In Vivo Toxicity Evaluation and Quantification of Iron Oxide Nanoparticles. *Inernational Journal of Molecular Sciences, 16,* 24417.
27. Fu, C., Liu, T., Li, L., Liu, H., Chen, D., Tang, F. (2013). The Absorption, Distribution, Excretion and Toxicity of Mesoporous Silica Nanoparticles in Mice Following Different Exposure Routes. *Biomaterials, 34,* 2565.
28. Li, M., Al-Jamal, K., Kostarelos, L., Reineke, J. (2010). Physiologically Based Pharmacokinetic Modeling of Nanoparticles. *ACS Nano, 4,* 6303.
29. Avgoustakis, K., Beletsi, A., Panagi, Z., Klepetsanis, P., Livaniou, E. Evangelatos, G., Ithakissios, D. (2003). Effect of Copolymer Composition on the the Physicochemical Characteristics, *in vitro* Stability and Biodistribution of PLGA-mPEG Nanoparticles. *International Journal of Pharmacology. 259.* 115-127.
30. DeFrates, K., Markiewicz, T., Gallo, P., Rack, A., Weyhmiller, A., Jarmusik, B., Hu, X. (2018). Protein Polymer-Based Nanoparticles: Fabrication and Medical Applications. *International Journal of Molecular Sciences. 19,* 1717.
31. Aubin-Tam, M. & Hamad-Schifferli, K. (2008). Structure and function of nanoparticle–protein conjugates. *Biomedical Materials, 3,* 034001.
32. Martin, L., Akhavan, B. & Bilek, M. (2018). Electric fields control the orientation of peptides irreversibly immobilized on radical-functionalized surfaces. *Nature Communications,* 9(357).
33. Sperling R. A. & Parak W. J. (2010). Surface modification, functionalization and bioconjugation of colloidal inorganic nanoparticles. *Philosophical Transactions of the Royal Society A: Mathematical, Physical and Engineering Sciences*. 368.
34. Maitre, J. & Heisenberg, C. (2013). Three Functions of Cadherins in Cell Adhesion. *Current biology, 23(*14*),* R626.
35. Stemmler, M. (2008). Cadherins in development and cancer. *Molecular Biosystems Journal*. 4. 835.
36. Van Roy, F. & Berx, G. (2008). The cell-cell adhesion molecule E-cadherin. *Cellular and Molecular Life Sciences, 65,* 3756.
37. Overduin M., Harvey T. S., Bagby S., Tong K. I., Yau P., Takeichi M. & Ikura M. (1995). Solution structure of the epithelial cadherin domain responsible for selective cell adhesion. *Science, 267,* 386.
38. Kim, S. A., Tai, C. Y., Mok, L. P., Mosser, E. A., & Schuman, E. M. (2011). Calcium-dependent dynamics of cadherin interactions at cell-cell junctions. *Proceedings of the National Academy of Sciences of the United States of America, 108(*24*),* 9857.
39. Schumann-Gillett, A., Mark, A. E., Deplazes, E., & O'Mara, M. L. (2017). A potential new, stable state of the E-cadherin strand-swapped dimer in solution. *European Biophysics Journal, 47(*1*),* 59.
40. Zhang YX, Sivasankar S, Nelson WJ, & Chu, S. (2009). Resolving cadherin interactions and binding cooperativity at the single-molecule level. *Proceeding of the National Academy of Sciences USA, 106,* 109.

41. Wu, Y., Jin, X., Harrison, O., Shapiro, L., Honig, B. & Ben-Shaul, A. (2010). Cooperativity between *trans* and *cis* interactions in cadherin-mediated junction formation. *Proceedings of the National Academy of Sciences, 107 (*41*),* 17592.
42. Pontani, L., Jorjadz, I. & Brujic, J. (2016). *Cis* and *Trans* cooperativity of E-cadherin mediates Adhesion in Biomimetic Lipid Droplets. *Biophysical Journal, 110*, 391.
43. Harrison, O. J., Bahna, F., Katsamba, P. S., Jin, X., Brasch, J., Vendome, J., & Shapiro, L. (2010). Two-step adhesive binding by classical cadherins. *Nature structural & molecular biology*, *17(3)*, 348.
44. Ying Li, Y., Altorelli, N., Bahna, F., Honig, B., Shapiro, L. & Palmer, A. (2013). Mechanism of E-cadherin dimerization probed by NMR relaxation dispersion. *Proceedings of the National Academy of Science USA, 110*, 16462.
45. Ozawa M (2002) Lateral dimerization of the E-cadherin extracellular domain is necessary but not suffcient for adhesive activity, *Journal of Biology and Chemistry, 277*, 19600.
46. Angioletti, S. (2018). Theory, simulations and the design of functionalized nanoparticles for biomedical applications: A Soft Matter Perspective. *Nature: Computational Materials, 3(48).*
47. Ji, X. & Wang, Y. (2016). METHOD: Conjugation Protocols for Magnetic Nanoparticles. Sigma-Aldrich Methods. Url: https://www.sigmaaldrich.com/content/dam/sigmaaldrich/docs/promo_NOT_INDEXED/General_Information/1/conjugation-protocols-formagneticnanoparticles.pdf. Visited: 05/28/2019.
48. Suk, J., Xu, Q., Kim, N., Hanes, J., Ensign, L. (2016). PEGylation as a strategy for improving nanoparticle-based drug and gene delivery. *Advanced Drug Delivery Reviews*, *99*(Pt A), 28.
49. Kwak, M., Gu, W., Jeong, H., Lee, H., Lee, J., An, M., Kim, Y., Lee, J., Cheon, J. & Jun, Y. (2019). Small, clickable, and monovalent magnetofluorescent nanoparticles (MFNs) enable mechanogenetic regulation of receptors in a crowded live cell microenvironment. *Nano Letters, 19*(6), 3761.
50. Geletua, M., Arulanandama, R., Chevalier, S., Saezc, N., Larued, L., Feracci, H. & Raptis, L. (2013). Classical cadherins control survival through the gp130/Stat3 axis, *Biochimica et Biophysica Acta (BBA) - Molecular Cell Research, 1833*(8), 1947.